

**Brane-induced Skymion on  $S^3$ : Baryonic matter in holographic QCD**

Kanabu Nawa\*

*Research Center for Nuclear Physics (RCNP), Osaka University, Mihogaoka 10-1, Ibaraki, Osaka 567-0047, Japan*Hideo Suganuma<sup>†</sup>*Department of Physics, Graduate School of Science, Kyoto University, Kitashirakawa, Sakyo, Kyoto 606-8502, Japan*Toru Kojo<sup>‡</sup>*RIKEN BNL Research Center, Brookhaven National Laboratory, Upton, New York 11973, USA*

(Received 7 October 2008; published 27 January 2009)

We study baryonic matter in holographic QCD with D4/D8/ $\overline{D8}$  multi-D brane system in type IIA superstring theory. The baryon is described as the “brane-induced Skymion,” which is a topologically nontrivial chiral soliton in the four-dimensional meson effective action induced by holographic QCD. We employ the “truncated-resonance model” approach for the baryon analysis, including pion and  $\rho$  meson fields below the ultraviolet cutoff scale  $M_{KK} \sim 1$  GeV, to keep the holographic duality with QCD. We describe the baryonic matter in large  $N_c$  as single brane-induced Skymion on the three-dimensional closed manifold  $S^3$  with finite radius  $R$ . The interactions between baryons are simulated by the curvature of the closed manifold  $S^3$ , and the decrease of the size of  $S^3$  represents the increase of the total baryon-number density in the medium in this modeling. We investigate the energy density, the field configuration, the mass and the root-mean-square radius of single baryon on  $S^3$  as the function of its radius  $R$ . We find a new picture of “pion dominance” near the critical density in the baryonic matter, where all the (axial) vector meson fields disappear and only the pion fields survive. We also find the swelling phenomena of the baryons as the precursor of the deconfinement, and propose the mechanism of the swelling in the general context of QCD. The properties of the deconfinement and the chiral symmetry restoration in the baryonic matter are examined by taking the proper order parameters. We also compare our truncated-resonance model with another instanton description of the baryon in holographic QCD, considering the role of cutoff scale  $M_{KK}$ .

DOI: [10.1103/PhysRevD.79.026005](https://doi.org/10.1103/PhysRevD.79.026005)

PACS numbers: 11.25.Uv, 12.38.–t, 12.39.Dc, 12.39.Fe

**I. INTRODUCTION**

The concept of “holography” was first introduced by D. Gabor in 1948 [1] as a new technique of the optical physics to playback the three-dimensional information onto the two-dimensional plate as a hologram. In 1997, this concept of holography got a new appearance in the framework of the superstring theory as the duality between two theories belonging to the different spatial dimensions. It is first proposed by Maldacena [2] as the AdS/CFT correspondence between  $AdS_5 \times S^5$  supergravity and  $\mathcal{N} = 4$  supersymmetric Yang-Mills theory through D3 brane in type IIB superstring theory. In a more general point of view, an essential element of the holography is “ $D_p$  brane” as the  $(p + 1)$ -dimensional membrane in the ten-dimensional space-time. In fact, the  $D_p$  brane appears as the soliton, i.e., the condensed object of the fundamental strings. The  $D_p$  brane has two important aspects as follows:  $(p + 1)$ -dimensional gauge theory appears *on* a surface of the  $D_p$  brane, and  $\{(p + 1) + 1\}$ -dimensional supergravity appears *around* the  $D_p$  brane. (The italic “ $I$ ” denotes the

radial dimension with nontrivial curvature around the  $D_p$  brane, indicating the existence of the gravity). Actually, the concept of holography indicates the duality between the  $(p + 1)$ -dimensional gauge theory without the gravity and  $\{(p + 1) + 1\}$ -dimensional supergravity mediated by the  $D_p$  brane, and the gauge interaction as a “hologram” on the surface of the  $D_p$  brane is to give the supergravity as a “vision” in the extra dimension.

One of the most essential properties of the holography is the “strong-weak duality” between the gauge theory and the supergravity: the coupling strengths are transversely related with each other. Therefore, the holography provides a remarkable possibility that nonperturbative aspects of one side can be analyzed by the other dual side just with the tree-level calculations. Then, if we find the special configurations of D branes reflecting QCD on their surfaces, nonperturbative aspects of QCD can be successfully examined from the tree-level dual supergravity side. This is the strategy of the holographic QCD.

There exist several trials to find the special configurations of D branes reflecting QCD. Eventually, in 2005, Sakai and Sugimoto succeeded in constructing QCD with massless quarks and gluons from the fluctuation modes of the open strings on the D4/D8/ $\overline{D8}$  multi-D brane configurations in type IIA superstring theory [3], called Sakai-

\*nawa@rcnp.osaka-u.ac.jp

†suganuma@ruby.scphys.kyoto-u.ac.jp

‡torujj@quark.phy.bnl.gov

Sugimoto model, which is one of the most realistic models of holographic QCD. By using this model, many phenomenological properties of *mesons* belonging to the nonperturbative aspects of QCD like meson mass spectra, hidden local symmetry [4], vector meson dominance [5], KSFR relation [6], GSW model [7], etc., are successfully derived from the tree-level dual supergravity calculations. In this sense, holographic QCD is often regarded as the “unified meson theory.” On the other hand, baryon description is not straightforward in this approach since the classical supergravity is found to be dual with the strong-coupling “large- $N_c$ ” QCD, where baryons do not directly appear as dynamical degrees of freedom [8].

In our previous work, we gave the first study of the baryon as a nontrivial topological soliton in the four-dimensional meson effective action derived from holographic QCD. We call this topological soliton as a “brane-induced Skyrmion” [9,10]. Especially we included pions and  $\rho$  mesons appearing below the Kaluza-Klein mass scale  $M_{\text{KK}} \sim 1$  GeV, which is often called the “truncated-resonance model” for the baryon analysis.

Actually,  $M_{\text{KK}}$  plays the role as the ultraviolet cutoff scale of the holographic approach. In fact, there appear an infinite number of “non-QCD modes” with mass scale  $\sim O(M_{\text{KK}})$  in holographic QCD like gluinos and Kaluza-Klein modes. In this sense, the duality with QCD could be maintained below  $M_{\text{KK}}$  as the ultraviolet cutoff.

The appearance of certain cutoff scale  $M_{\text{KK}}$  should be essential for the holographic approach to be dual of realistic QCD with confinement and chiral symmetry breaking as the non-SUSY natures. In the holographic model with D4/D8/ $\overline{\text{D8}}$  multi-D brane system, D4 branes are  $S_1$ -compactified with the  $M_{\text{KK}}$  scale, to give the complete SUSY breaking and its resulting nonconformal natures of QCD, like finite string tension and chiral condensate. These considerations suggest that  $M_{\text{KK}}$  should be well respected, giving our truncation of meson resonances at  $M_{\text{KK}}$  for baryon analysis (See, Sec. II for details).

Recently a baryon is also described as an instanton on the five-dimensional gauge theory of D8 branes with D4 supergravity background [11–15]. The instanton is introduced *before* the mode expansion of the five-dimensional gauge field into mesons, so that the baryon as the instanton is to be composed by the infinite number of color-singlet modes with the mesonic quantum number even above the  $M_{\text{KK}}$  scale. However, we consider that such color-singlet modes above  $M_{\text{KK}}$  might not directly correspond to physical mesons in QCD, because the duality with QCD is maintained below  $M_{\text{KK}}$ . Furthermore, there also exists an infinite number of other non-QCD modes above  $M_{\text{KK}}$ , which could also affect the baryon properties if they were included. Therefore, in contrast to instanton models, we severely respect the cutoff scale  $M_{\text{KK}}$  and truncate the meson resonances at  $M_{\text{KK}}$  to keep the duality with QCD. More comprehensive discussions with instantons are summarized in Sec. VII.

In the present work, we newly consider the extension of the holographic model to dense QCD. Because of the non-Abelian nature of QCD, various realizations are expected in the vacuum itself with finite temperature and density, called “QCD phase diagram.” Up to now, interesting phase structures are proposed by using some low-energy effective theories of QCD, e.g., a confined phase with mesons and baryons, a deconfined phase with quark-gluon plasma (QGP), a chiral symmetry broken phase with mass generation [16], color superconductivity as diquark condensation [17–21], etc. In fact, some wisdom about QGP gives the insight for the early universe just after the big bang [22]. Furthermore, the possible QCD phase transitions in the core region of neutron stars could affect a lot of their macroscopic features like moment of inertia, angle velocity, and breaking index [23]. There also exist several experimental projects to search the QGP in the ultrarelativistic heavy ion collisions in the RHIC (Relativistic Heavy Ion Collider) at BNL, and the LHC at CERN. There will also appear relatively low-energy collision experiments to make the low-temperature high-density object in FAIR (Facility for Antiproton and Ion Research) at GSI, giving some knowledge about the core region of the compact stars. With these backgrounds, it should be urgently important to make clear the structure of the QCD phase diagram more explicitly from QCD itself with the rich help of experimental data, which will eventually bring about the fundamental understanding of our whole nature.

There exists the lattice QCD numerical study as the first principle calculation of the strong interaction. However, because of the “sign problem,” its applicability is severely restricted near the zero-density at finite-temperature regime of the wide QCD phase diagram (For some review, see, Ref. [24]). Therefore, if one succeeds in the extension of holographic approach to the dense regime, it should give a new analytical tool for nonperturbative aspects of the finite density QCD, where the holography provides the duality between the strong-coupling gauge theory and the weak-coupling supergravity. This is the main aim of our study.

In this work, we consider the baryonic matter in holographic QCD as the extension of the holographic approach to dense QCD. Especially, we treat the baryonic matter with large- $N_c$  because the holographic QCD is derived as a large- $N_c$  effective theory. As the general property of large- $N_c$  QCD [8], the static baryon mass is proportional to  $O(N_c)$ , so that its kinetic energy becomes  $O(N_c^{-1})$ . There also exist the quantum effects like the zero point quantum fluctuation energy  $E_0$  and also the baryon mass splitting  $\Delta m$  within the baryonic matter, while these correspond to the higher order contributions of the  $1/N_c$  expansions as  $E_0 \sim O(N_c^0)$  and  $\Delta m \sim O(N_c^{-1})$  [25]. Such large- $N_c$  countings indicate that, for sufficiently large  $N_c$ , the kinetic energy and the quantum effects within the baryonic matter can be suppressed relative to the static mass, and the

baryonic matter comes into the static Skyrme matter. Such static Skyrme matter was first analyzed by Klebanov [26], by placing the Skyrme soliton solutions periodically along the three-dimensional cubic lattice, which would correspond to the nuclear crystal in the deeper interior of neutron stars.

Since the cubic lattice treatment is rather cumbersome, we employ a mathematical trick to analyze such static Skyrme matter, proposed by Manton and Ruback [27]. In order to represent some high-density state of the multi-Skyrmion system on the three-dimensional flat space  $\mathbf{R}^3$ , single Skyrme is alternately placed on a surface of the three-dimensional closed manifold  $S^3$  with a finite radius. In fact, the multi-Skyrmion system on  $\mathbf{R}^3$  and the single Skyrme on  $S^3$  can be related with each other through the compactification of the boundary of a unit cell on  $\mathbf{R}^3$  shared by one Skyrme. The interactions between baryons on  $\mathbf{R}^3$  are simulated by the curvature of the manifold  $S^3$ , and decreasing the radius of  $S^3$  represents the increase of the baryon-number density in the medium in this modeling. Actually, by taking such mathematical simplification, one could avoid some complicated analysis like Monte Carlo simulations on the three-dimensional cubic lattice [26], and he can get some physical intuitions as for the baryonic matter qualitatively and even quantitatively [27]. Therefore, by placing the single brane-induced Skyrme on the closed manifold  $S^3$ , we try to analyze the typical features of baryonic matters in holographic QCD. Especially, in this analysis, the roles of  $\rho$  mesons in the dense baryonic matter will be examined in detail from the holographic point of view.

There exist a lot of works about the extension of the holographic approaches to dense SUSY QCD (See, Ref. [28] and references therein). With the bottom-up construction of the AdS/QCD models [29–36], it was applied to dense QCD by introducing the bi-nucleon condensate [37]. After the discovery of the Sakai-Sugimoto model [3] as one of the most reliable holographic top-down approaches to non-SUSY QCD with massless quark flavors, there exist several proposals about the extension of this model to dense QCD. For example, in Refs. [38,39], the baryon chemical potential  $\mu_B$  is introduced by the asymptotic value of a  $U(1)$  gauge field on the D8- $\overline{\text{D8}}$  branes as  $\mathcal{V}_0 = -i\mu_B/N_c$ , similarly to the introduction of the chemical potentials to the chiral perturbation theory by promoting the global chiral symmetry to local gauge one [40,41]. In these holographic analyses, the density dependence of the “local” properties of mesons and baryons like their masses and coupling constants, and also the phase structure of QCD have been successfully discussed. Now, in our paper, we treat the baryon as a “nonlocal” solitonic object as the Skyrme in the Sakai-Sugimoto model, and we analyze the dense QCD by the Skyrme matter. Therefore, adding to the information about the local natures of hadrons and QCD phase structure, we can ex-

tensively examine the internal structure of the baryon, e.g. the size and the field configurations.

Here we show the organization of this paper and its brief summary. In Sec. II, we overview the holographic derivation of the four-dimensional meson effective action with the pion and  $\rho$  meson fields, reemphasizing the role of cutoff scale  $M_{\text{KK}}$  in the holographic framework to be dual of QCD. In Sec. III, we analyze the properties of baryons and baryonic matter in holographic QCD. In Sec. III A, we introduce the concept of the brane-induced Skyrme on the three-dimensional flat space  $\mathbf{R}^3$ . Then, in Sec. III B, we describe the baryonic matter as the system of single brane-induced Skyrme on the three-dimensional closed manifold  $S^3$ . We derive the expression of the hedgehog mass and Euler-Lagrange equations for the pion and  $\rho$  meson fields as the brane-induced Skyrme on  $S^3$ . Section IV is devoted to the numerical results and their physical interpretations about the baryon nature in dense QCD. In Sec. IV A, the baryon-number density dependence of the energy density and field configuration profiles of a single baryon are discussed. In Sec. IV B, we propose a new striking picture of the “pion dominance” near the critical density, i.e., all the (axial) vector meson fields disappear and only the pion field survives. In Sec. IV C, the baryon-number density dependence of the mass and root-mean-square mass radius of the single baryon are analyzed. We find some nonlinear increase in the size of the baryon near the critical density as swelling phenomena. In Sec. IV D, we explain the swelling mechanism in the general context of QCD, and consider its effects on the stability of  $N$ - $\Delta$  mixed matter. In Sec. V, we examine the features of the delocalization phase transitions and the chiral symmetry restoration by choosing proper order parameters, through which the relations between deconfinement and chiral symmetry restoration are reconsidered. In Sec. VI, we calculate the critical densities of the phase transitions in the physical units with the experimental inputs for the pion decay constant  $f_\pi (= 92.4 \text{ MeV})$  and  $\rho$  meson mass  $m_\rho (= 776.0 \text{ MeV})$ . We find the critical density  $\rho_B \simeq 7\rho_0$  in the holographic approach. Through all of the sections, by comparing the brane-induced Skyrme and standard Skyrme without  $\rho$  meson fields, the roles of the vector mesons in the dense baryonic matter are examined from the holographic point of view. Sec. VII is devoted to summary and outlook. In this final section, we compare our truncated-resonance approach with another instanton description of baryons [11–15] in the holographic QCD, paying attention on the role of cutoff scale  $M_{\text{KK}}$ .

## II. MESON EFFECTIVE THEORY FROM HOLOGRAPHIC QCD

In this section, we overview the derivation of the four-dimensional meson effective action from holographic QCD with the D4/D8/ $\overline{\text{D8}}$  multi-D brane system in type IIA superstring theory, called the Sakai-Sugimoto model

[3]. The meson effective action is derived without small amplitude expansion to discuss a baryon as a large amplitude chiral soliton. (For more comprehensive derivations, see our previous paper [9]). Here we especially emphasize the roles of cutoff scale  $M_{\text{KK}}$  in holographic QCD.

First, we review the construction of the D4/D8/ $\overline{\text{D8}}$  multi-D brane system and also the supergravity description of D4 branes as the holographic dual of QCD. As the first step,  $N_c$  sheets of D4 branes are prepared to construct the gluon sector of QCD. The D4 branes are  $S^1$ -compactified along one extra dimension with a radius as the inverse of the Kaluza-Klein mass scale  $M_{\text{KK}}$ . There appear ten independent fluctuation modes from the open strings on the surface of D4 branes, i.e., gauge fields  $\mathcal{A}_{\mu=0\sim 3}$ , scalar fields  $A_4$  and  $\Phi_{i=5\sim 9}$ , and also their superpartners as fermions. By imposing the antiperiodic boundary conditions for all the fermions along the  $S^1$ -compactified direction, they acquire large masses  $\sim O(M_{\text{KK}})$ . Then supersymmetry (SUSY) is completely broken and, due to the radiative corrections, all the scalar fields  $A_4$  and  $\Phi_i$  also get large masses  $\sim O(M_{\text{KK}})$ . Because of the  $S^1$ -compactification, there also appear the infinite number of the Kaluza-Klein modes with masses  $\sim O(M_{\text{KK}})$ . Therefore, below the  $M_{\text{KK}}$  scale, only massless gauge fields  $\mathcal{A}_\mu$  appear. In this sense, the system of  $N_c$  sheets of D4 branes with the  $S^1$ -compactification can be viewed as the  $U(N_c)$  Yang-Mills theory below  $M_{\text{KK}}$  scale, corresponding to the pure gauge sector of QCD. As the next step,  $N_f$  sheets of D8 and  $\overline{\text{D8}}$  branes are added to introduce the massless quark flavors of QCD.  $\overline{\text{D8}}$  has opposite chirality relative to D8, providing  $U(N_f)_L \times U(N_f)_R$  chiral symmetry in this model. From the fluctuation modes of open strings between D4 and D8 ( $\overline{\text{D8}}$ ), there appear massless chiral fermions as quarks in QCD. As a whole, massless QCD appears as the hologram on the surface of D4/D8/ $\overline{\text{D8}}$  branes.

Then we shift into the gravitational description of D branes from the extra dimensions. The D brane is originally introduced as the fixed edges of open strings with Dirichlet boundaries. This also indicates that, through the ‘‘open-closed duality’’ for the fundamental strings, the D brane can also be regarded as the source of closed strings, giving the graviton in the extra dimensions outside of the D brane. In this sense, the D brane can be identified as a highly gravitational system, i.e., the ‘‘black brane,’’ allowing the gravitational description from the extra dimensions. In fact, the mass of the D branes is proportional to its sheets number, so that, by assuming  $N_c \gg N_f$ , only D4 branes can be represented by the gravitational background and D8 ( $\overline{\text{D8}}$ ) branes are introduced as the probes called ‘‘probe approximation,’’ which corresponds to the quenched approximation in lattice QCD study [42]. Especially the classical supergravity description of D4 branes is tractable, followed by the local approximation of the strings and also the suppressions of the string loop effect. These conditions in the gravitational side around the D branes give the

constraints for the gauge theory side as the QCD on the surface of D branes as

$$g_{\text{YM}}^4 \ll \frac{1}{g_{\text{YM}}^2 N_c} \ll 1, \quad (1)$$

which is achieved by  $g_{\text{YM}} \rightarrow 0$ ,  $N_c \rightarrow \infty$ , and 'tHooft coupling:  $\lambda \equiv g_{\text{YM}}^2 N_c$  fixed and large. In this sense, the strong-coupling large- $N_c$  QCD is found to be dual with the classical supergravity of D4 branes with probe D8 ( $\overline{\text{D8}}$ ) branes, which is one of the realizations of the strong-weak duality between the gauge theory and gravitational theory through the holography. Therefore, by analyzing the effective action of D8 branes with D4 supergravity background, one can analyze the nonperturbative aspects of QCD on the surface of D branes.

Then we start formal discussions from the  $N_f = 2$  non-Abelian Dirac-Born-Infeld (DBI) action of probe D8 brane with D4 supergravity background as a probe approximation. After dimensional reductions, the nine-dimensional DBI action of the probe D8 brane with the D4 supergravity background can be reduced into a five-dimensional Yang-Mills theory, belonging to the flat four-dimensional Euclidean space-time  $x$ , i.e.,  $x_{0\sim 3}$  and the other fifth dimension  $z$  with curved measures as follows [3]:

$$S_{\text{D8}}^{\text{DBI}} - S_{\text{D8}}^{\text{DBI}}|_{A_M \rightarrow 0} = \kappa \int d^4 x dz \text{tr} \left\{ \frac{1}{2} K(z)^{-1/3} F_{\mu\nu} F_{\mu\nu} + K(z) F_{\mu z} F_{\mu z} \right\} + O(F^4), \quad (2)$$

where  $A_M$  is the gauge field and  $F_{MN} = \partial_M A_N - \partial_N A_M + i[A_M, A_N]$  ( $M, N = 0 \sim 3, z$ ) is the field strength tensor in five-dimensional space-time  $(x_{0\sim 3}, z)$  of the probe D8 branes. In the action (2),  $M_{\text{KK}} = 1$  unit is taken, and the overall factor  $\kappa$  is defined as

$$\kappa \equiv \frac{\lambda N_c}{216\pi^3}. \quad (3)$$

(Note here that we use the value of  $\kappa$  as a half of that in Ref. [9], taking away the misleading factor 2 in Eq. (16) of Ref. [9]. All the formulas and numerical results can be scaled by the factor  $\kappa$ , so that the discussions in Ref. [9] are not altered.) The functional  $K(z) \equiv 1 + z^2$  in the action (2) expresses the nontrivial curvature in the extra fifth dimension  $z$  induced by the supergravity background of the D4 brane. The gravitational energy of the D8 brane, i.e.,  $S_{\text{D8}}^{\text{DBI}}|_{A_M \rightarrow 0}$  is subtracted in the action (2) as the vacuum relative to the gauge sectors.

In the D4/D8/ $\overline{\text{D8}}$  multi-D brane configurations, color quantum number is carried only by the  $N_c$  sheets of D4 branes. Therefore, after the supergravity description of D4 branes, there are no colored particles from the fluctuation modes of open strings on the residual probe D8 branes. This is regarded as some holographic manifestation of ‘‘color confinement’’ in the low-energy scale of QCD. In fact, gauge field  $A_{M=0\sim 3, z}$  in the action (2) is a color-singlet

and obeys the adjoint representation of the  $U(N_f)$  group, eventually producing the meson degrees of freedom after some proper mode expansions in the holographic QCD.

In this paper, we treat the nontrivial leading order of  $1/N_c$  and  $1/\lambda$  expansions in the holographic QCD as the five-dimensional Yang-Mills action (2) with  $O(F^2)$ . In general, there also exists the Chern-Simons (CS) term to avoid anomalies in the superstring theory. By introducing  $\omega$  meson degrees of freedom as the  $U(1)$  sector of  $\rho$  meson fields in the holographic approach, the  $\omega$  meson indirectly couples with pions via (axial) vector mesons after the proper mode expansions of CS term, which is regarded as a general representation of the Gell-Mann–Sharp–Wagner (GSW) model [7]. The roles of  $\omega$  mesons for low-energy meson dynamics and also chiral solitons have been traditionally examined in some QCD phenomenologies [43]. Actually, however, the CS term is found to be  $O(\lambda^0)$ , i.e., the higher order contributions of 'tHooft coupling expansion relative to the  $O(F^2)$  of the Yang-Mills action (2) with  $O(\lambda^1)$ , which is manifestly shown in holographic QCD. Furthermore, the majority of the CS term includes one time-derivative of pion fields and does not affect the static properties of hedgehog solitons. Therefore, we neglect the CS term in the discussions below for the argument of the nonperturbative (strong coupling) properties of QCD.

In the holographic approach, the pion field is introduced as the Wilson line of the fifth gauge field  $A_z$ , i.e., a path-ordered product of the fifth gauge field along the  $z$  direction [3,9,31] as

$$U(x^\mu) = P \exp \left\{ -i \int_{-\infty}^{\infty} dz' A_z(x_\mu, z') \right\} \in U(N_f). \quad (4)$$

One can also introduce the variables  $\xi_\pm(x_\mu)$  as

$$\xi_\pm^{-1}(x^\mu) = P \exp \left\{ -i \int_{z_0(x_\mu)}^{\pm\infty} dz' A_z(x_\mu, z') \right\} \in U(N_f), \quad (5)$$

where  $z_0(x_\mu)$  is a single-valued arbitrary function of  $x_\mu$ . Then the pion field (4) can be written as

$$U(x^\mu) = \xi_+^{-1}(x_\mu) \xi_-(x_\mu), \quad (6)$$

some resemble formulas which can also be found in the traditional approach of hidden local symmetry [4].

Now we take “ $A_z = 0$  gauge” and also “ $\xi_+^{-1}(x_\mu) = \xi_-(x_\mu)$  ( $\equiv \xi(x_\mu)$ ) gauge” for the  $U(N_f)$  gauge symmetry in the action (2) of the probe D8 brane. The  $A_z = 0$  gauge is similar to the unitary gauge in the non-Abelian Higgs theory; fifth gauge field  $A_z$  performs as a scalar field in four-dimensional space-time  $x_{\mu=0\sim 3}$ , and it is eaten by the four-dimensional gauge field  $A_\mu$  to give the mass generation of gauge field, especially the (axial) vector mesons as a part of  $A_\mu$ . In this sense the masses of the (axial) vector mesons come from the Higgs mechanism in five-dimensional space-time with the  $U(N_f)$  gauge sym-

metry breaking on the probe D8 brane. The  $\xi_+^{-1}(x_\mu) = \xi_-(x_\mu)$  gauge is also essential to get the low-energy effective theory of QCD with proper parity and G-parity classification in a manifest way [9]. With these gauge fixings, the five-dimensional gauge field  $A_\mu(x_N)$  can be mode-expanded into the four-dimensional parity and G-parity eigenstates with proper complete orthogonal basis  $\psi_\pm(z)$  and  $\psi_n(z)$  ( $n = 1, 2, \dots$ ) as follows [3,9]:

$$A_\mu(x_N) = l_\mu(x_\nu) \psi_+(z) + r_\mu(x_\nu) \psi_-(z) + \sum_{n \geq 1} B_\mu^{(n)}(x_\nu) \psi_n(z), \quad (7)$$

$$l_\mu(x_\nu) \equiv \frac{1}{i} \xi^{-1}(x_\nu) \partial_\mu \xi(x_\nu), \quad (8)$$

$$r_\mu(x_\nu) \equiv \frac{1}{i} \xi(x_\nu) \partial_\mu \xi^{-1}(x_\nu), \quad (9)$$

where  $l_\mu$  and  $r_\mu$  are left and right currents of pion fields, respectively. The basis  $\psi_\pm(z)$  are introduced to support whole of the gauge field  $A_\mu(x_N)$  at the boundary  $z \rightarrow \pm\infty$  as  $\psi_\pm(z \rightarrow \pm\infty) = 1$  and  $\psi_\pm(z \rightarrow \mp\infty) = 0$  as

$$\psi_\pm(z) \equiv \frac{1}{2} \pm \hat{\psi}_0(z), \quad (10)$$

$$\hat{\psi}_0(z) \equiv \frac{1}{\pi} \arctan z. \quad (11)$$

In order to diagonalize the five-dimensional Yang-Mills action (2) with the induced measures  $K(z)^{-1/3}$  and  $K(z)$  in the fifth dimension  $z$ , the basis  $\psi_n$  ( $n = 1, 2, \dots$ ) are taken to be the normalizable eigenfunction satisfying

$$-K(z)^{1/3} \frac{d}{dz} \left\{ K(z) \frac{d\psi_n}{dz} \right\} = \lambda_n \psi_n, \quad (\lambda_1 < \lambda_2 < \dots) \quad (12)$$

with normalization condition as

$$\kappa \int dz K(z)^{-1/3} \psi_m \psi_n = \delta_{nm}. \quad (13)$$

In the holographic model, the fields  $B_\mu^{(n=1,2,\dots)}$  in the mode expansion (7) are regarded as (axial) vector mesons, belonging to the adjoint representation of the  $U(N_f)$  gauge group as  $B_\mu = B_\mu^a T^a$ . By substituting the expansion (7) into the action (2), the mass of  $B_\mu^{(n)}$  field is found with the eigenvalue of oscillating fifth basis in Eq. (12) as  $m_n^2 \equiv \lambda_n$ , indicating that the origin of meson mass is the oscillation of meson wave function in the extra fifth dimension. Furthermore,  $A_\mu(x_N)$  is the five-dimensional vector and  $\psi_n(z)$  are the parity eigenstate in the  $z$  direction as  $\psi_n(-z) = (-)^{n-1} \psi_n(z)$ . Therefore, from the mode expansion (7),  $B_\mu^{(n)}$  fields have four-dimensional parity transformation as  $B_\mu^{(n)}(-x_\nu) \rightarrow (-)^n B_\mu^{(n)}(x_\nu)$ . These consideration indicates that vector and axial vector mesons

appear alternately in the excitation spectra about index  $n$  as  $B_\mu^{(1)} \equiv \rho_\mu, B_\mu^{(2)} \equiv a_{1\mu}, B_\mu^{(3)} \equiv \rho'_\mu, B_\mu^{(4)} \equiv a'_{1\mu}, B_\mu^{(5)} \equiv \rho''_\mu, \dots$ .

In our study, we construct the four-dimensional meson effective action only with pion field  $U(x_\nu)$  and  $\rho$  meson field  $B_\mu^{(1)}(x_\nu) \equiv \rho_\mu(x_\nu)$  below the Kaluza-Klein mass scale  $M_{\text{KK}} \sim 1$  GeV. Recall that there appears an infinite number of non-QCD modes with large mass  $\sim O(M_{\text{KK}})$  in holographic QCD, e.g., scalar fields, gluino, and also the Kaluza-Klein modes, discussed in the first part of this section. Therefore, the D4/D8/ $\overline{\text{D8}}$  multi-D brane system can be viewed as QCD as far as low-energy phenomenology below  $\sim M_{\text{KK}}$  is concerned. In this sense,  $M_{\text{KK}}$  plays the roles as the ultraviolet cutoff scale of the theory, so that we include the meson degrees of freedom below  $M_{\text{KK}}$  for the baryon analysis in later sections, called ‘‘truncated-resonance model.’’

Actually, the appearance of  $M_{\text{KK}}$  scale with finite value seems to be essential in the recent holographic analysis. In the framework of AdS/CFT correspondence without Kaluza-Klein compactification, the  $\mathcal{N} = 4$  SUSY and its resulting conformal symmetry protect the emergence of the dimensional quantities like string tension and chiral condensate at the ground state, because of the cancellation of the radiative corrections between bosons and fermions. In this sense, SUSY breaking is at least needed to be dual of QCD with confinement and chiral symmetry breaking as its vacuum nature. In the Sakai-Sugimoto model,  $N_c$  sheets of D4 branes are Kaluza-Klein compactified with radius  $M_{\text{KK}}^{-1}$ , and the SUSY is completely broken by the field boundary condition along the compactified direction. Therefore, confinement and chiral symmetry breaking *could* occur as the non-SUSY gauge theory. In fact, the compactified D4 brane is ‘‘non-BPS,’’ having a ‘‘horizon’’ in the supergravity description. In the holographic framework, confinement and chiral symmetry breaking *do* occur on this horizon,

giving the loss of ‘‘colored’’ information, and also the geometrical connection of D8 and  $\overline{\text{D8}}$  branes. As a whole, the appearance of  $M_{\text{KK}}$  would be essential for the holographic model to be dual of realistic QCD.

Now, one may regret about the finiteness of  $M_{\text{KK}}$  as almost 1 GeV, which is comparable with the QCD mass scale  $\Lambda_{\text{QCD}}$ . In the holographic approach, the QCD mass scale is introduced by the experimental inputs for the pion decay constant and  $\rho$  meson mass as  $f_\pi = 92.4$  MeV and  $m_\rho = 776.0$  MeV. These experimental values come from our hadronic world with  $N_c = 3$  and large but finite 'tHooft coupling  $\lambda$ , which may infringe the condition (1) to give the effects of string length and string loops in the gravitational side. Therefore, too large  $M_{\text{KK}}$  cannot be taken to neglect the internal structure of strings on the surface of D4 branes compactified with radius  $M_{\text{KK}}^{-1}$ , which might eventually give the scale  $M_{\text{KK}} \sim 1$  GeV. These considerations indicate that, by including the effects of string length and loops in the gravitational side,  $M_{\text{KK}}$  could be taken sufficiently large relative to  $\Lambda_{\text{QCD}}$  with fixed  $f_\pi$  and  $m_\rho$ . Anyway,  $M_{\text{KK}} \sim 1$  GeV essentially appears as the ultraviolet cutoff scale in the system of probe D8 brane with D4 ‘‘classical’’ supergravity background to be dual of QCD with proper dimensional quantities.

By neglecting the higher mass excitation modes of (axial) vector mesons rather than the  $\rho$  meson sector with  $n = 1$  in the expansions (7), the five-dimensional gauge field  $A_\mu(x_N)$  can be written as

$$A_\mu(x_N) = l_\mu(x_\nu)\psi_+(z) + r_\mu(x_\nu)\psi_-(z) + \rho_\mu(x_\nu)\psi_1(z). \quad (14)$$

By taking this mode expansion (14) with the  $A_z = 0$  gauge, five-dimensional field strength  $F_{\mu\nu}$  and  $F_{z\mu}$  can be written as

$$\begin{aligned} F_{\mu\nu} &= \partial_\mu A_\nu - \partial_\nu A_\mu + i[A_\mu, A_\nu] \\ &= (\partial_\mu l_\nu - \partial_\nu l_\mu)\psi_+ + (\partial_\mu r_\nu - \partial_\nu r_\mu)\psi_- + (\partial_\mu \rho_\nu - \partial_\nu \rho_\mu)\psi_1 + i\{[l_\mu, l_\nu]\psi_+^2 + [r_\mu, r_\nu]\psi_-^2 + [\rho_\mu, \rho_\nu]\psi_1^2\} \\ &\quad + i\{([l_\mu, r_\nu] + [r_\mu, l_\nu])\psi_+\psi_- + ([l_\mu, \rho_\nu] + [\rho_\mu, l_\nu])\psi_+\psi_1 + ([r_\mu, \rho_\nu] + [\rho_\mu, r_\nu])\psi_-\psi_1\} \\ &= -i[\alpha_\mu, \alpha_\nu]\psi_+\psi_- + (\partial_\mu \rho_\nu - \partial_\nu \rho_\mu)\psi_1 + i[\rho_\mu, \rho_\nu]\psi_1^2 + i\{([\alpha_\mu, \rho_\nu] + [\rho_\mu, \alpha_\nu])\hat{\psi}_0\psi_1 \\ &\quad + ([\beta_\mu, \rho_\nu] + [\rho_\mu, \beta_\nu])\psi_1\}, \end{aligned} \quad (15)$$

$$F_{z\mu} = \partial_z A_\mu = \alpha_\mu \partial_z \hat{\psi}_0 + \rho_\mu \partial_z \psi_1, \quad (16)$$

with axial-vector current  $\alpha_\mu$  and vector current  $\beta_\mu$  of the pion field as

$$\alpha_\mu(x_\nu) \equiv l_\mu(x_\nu) - r_\mu(x_\nu), \quad (17)$$

$$\beta_\mu(x_\nu) \equiv \frac{1}{2}\{l_\mu(x_\nu) + r_\mu(x_\nu)\}. \quad (18)$$

In the derivation of (15) and (16), we have used the Maurer-Cartan equations,  $\partial_\mu l_\nu - \partial_\nu l_\mu + i[l_\mu, l_\nu] = 0$  and  $\partial_\mu r_\nu - \partial_\nu r_\mu + i[r_\mu, r_\nu] = 0$ . By substituting Eqs. (15) and (16) into the five-dimensional Yang-Mills action (2) with  $O(F^2)$ , we eventually get the four-dimensional Euclidean meson effective action with pions and  $\rho$  mesons from holographic QCD as follows (derivations in more detail can be found in our previous paper [9]):

$$S_{\text{eff}} \equiv S_{\text{D8}}^{\text{DBI}} - S_{\text{D8}}^{\text{DBI}}|_{A_M \rightarrow 0} = \kappa \int d^4x dz \text{tr} \left\{ \frac{1}{2} K(z)^{-1/3} F_{\mu\nu} F_{\mu\nu} + K(z) F_{\mu z} F_{\mu z} \right\} \quad (19)$$

$$\begin{aligned} &= \frac{f_\pi^2}{4} \int d^4x \text{tr}(L_\mu L_\mu) + m_\rho^2 \int d^4x \text{tr}(\rho_\mu \rho_\mu) - \frac{1}{32e^2} \int d^4x \text{tr}[L_\mu, L_\nu]^2 + \frac{1}{2} \int d^4x \text{tr}(\partial_\mu \rho_\nu - \partial_\nu \rho_\mu)^2 \\ &+ i g_{3\rho} \int d^4x \text{tr}\{(\partial_\mu \rho_\nu - \partial_\nu \rho_\mu)[\rho_\mu, \rho_\nu]\} - \frac{1}{2} g_{4\rho} \int d^4x \text{tr}[\rho_\mu, \rho_\nu]^2 - i g_1 \int d^4x \text{tr}\{[\alpha_\mu, \alpha_\nu](\partial_\mu \rho_\nu - \partial_\nu \rho_\mu)\} \\ &+ g_2 \int d^4x \text{tr}\{[\alpha_\mu, \alpha_\nu][\rho_\mu, \rho_\nu]\} + g_3 \int d^4x \text{tr}\{[\alpha_\mu, \alpha_\nu](\beta_\mu, \rho_\nu) + [\rho_\mu, \beta_\nu]\} \\ &+ i g_4 \int d^4x \text{tr}\{(\partial_\mu \rho_\nu - \partial_\nu \rho_\mu)(\beta_\mu, \rho_\nu) + [\rho_\mu, \beta_\nu]\} - g_5 \int d^4x \text{tr}\{[\rho_\mu, \rho_\nu](\beta_\mu, \rho_\nu) + [\rho_\mu, \beta_\nu]\} \\ &- \frac{1}{2} g_6 \int d^4x \text{tr}([\alpha_\mu, \rho_\nu] + [\rho_\mu, \alpha_\nu])^2 - \frac{1}{2} g_7 \int d^4x \text{tr}([\beta_\mu, \rho_\nu] + [\rho_\mu, \beta_\nu])^2, \end{aligned} \quad (20)$$

where  $L_\mu$  is the 1-form of pion fields as

$$L_\mu(x_\nu) \equiv \frac{1}{i} U^\dagger(x_\nu) \partial_\mu U(x_\nu). \quad (21)$$

There exist 12 kinds of coupling constants:  $f_\pi$ ,  $m_\rho$ ,  $e$ ,  $g_{3\rho}$ ,  $g_{4\rho}$ , and  $g_{1-7}$  in the action (20). However, all of the coupling constants are uniquely determined from the properties of meson wave functions in the extra fifth dimension  $z$ , i.e., the complete orthogonal basis  $\psi_\pm(z)$  and  $\psi_1(z)$  with oscillating eigenvalue  $\lambda_1$  as follows:

$$\frac{f_\pi^2}{4} \equiv \kappa \int dz K(z) (\partial_z \hat{\psi}_0)^2 = \frac{\kappa}{\pi}, \quad (22)$$

$$m_\rho^2 \equiv m_1^2 = \lambda_1, \quad (23)$$

$$\frac{1}{16e^2} \equiv \kappa \int dz K(z)^{-1/3} \psi_+^2 (1 - \psi_+)^2, \quad (24)$$

$$g_{3\rho} \equiv \kappa \int dz K(z)^{-1/3} \psi_1^3, \quad (25)$$

$$g_{4\rho} \equiv \kappa \int dz K(z)^{-1/3} \psi_1^4, \quad (26)$$

$$g_1 \equiv \kappa \int dz K(z)^{-1/3} \psi_1 \psi_+ \psi_-, \quad (27)$$

$$g_2 \equiv \kappa \int dz K(z)^{-1/3} \psi_1^2 \left( \frac{1}{4} - \hat{\psi}_0^2 \right), \quad (28)$$

$$g_3 \equiv \kappa \int dz K(z)^{-1/3} \psi_1 \psi_+ \psi_- = g_1, \quad (29)$$

$$g_4 \equiv \kappa \int dz K(z)^{-1/3} \psi_1^2 = 1, \quad (30)$$

$$g_5 \equiv \kappa \int dz K(z)^{-1/3} \psi_1^3 = g_{3\rho}, \quad (31)$$

$$g_6 \equiv \kappa \int dz K(z)^{-1/3} \psi_1^2 \hat{\psi}_0^2 = \frac{1}{4} - g_2, \quad (32)$$

$$g_7 \equiv \kappa \int dz K(z)^{-1/3} \psi_1^2 = 1. \quad (33)$$

The holographic model has two parameters  $\kappa (= \frac{\lambda N_c}{216\pi^3})$  and the Kaluza-Klein mass  $M_{\text{KK}}$  as the ultraviolet cutoff scale of this theory.  $\kappa$  appears in front of the effective action (2) because the effective action of the D8 brane with a D4 supergravity background expanded up to  $O(F^2)$  corresponds to the leading order of  $1/N_c$  and  $1/\lambda$  expansions. Therefore, by fixing two parameters  $\kappa$  and  $M_{\text{KK}}$  to adjust experimental inputs for  $f_\pi$  and  $m_\rho$ , then all the coupling constants (22)–(33) are uniquely determined through the background of the extra fifth dimension  $z$ . Such uniqueness of the action is one of the remarkable consequences in holographic QCD.

### III. BRANE-INDUCED SKYRMION ON $\mathbf{R}^3$ AND $S^3$

In this section, we discuss baryons and baryonic matter in holographic QCD. In Sec. III A, we describe the baryon as a chiral soliton in the four-dimensional meson effective action  $S_{\text{eff}}$  in (20) including pion and  $\rho$  meson fields derived from holographic QCD. We call this topological soliton as the ‘‘brane-induced Skyrmion.’’ The hedgehog mass of the brane-induced Skyrmion on the flat coordinate space  $\mathbf{R}^3$  is derived, which is originally given in our previous paper [9]. In Sec. III B, we newly discuss the baryonic matter in holographic QCD by analyzing the system of the single brane-induced Skyrmion on the three-dimensional closed manifold  $S^3$ . Through the projection procedure from the flat space  $\mathbf{R}^3$  onto the curved space  $S^3$ , the hedgehog mass and the Euler-Lagrange equations of the brane-induced Skyrmion on  $S^3$  are derived. All the numerical results and their physical interpretations are presented in Secs. IV, V, and VI.

### A. Brane-induced Skyrmion on $\mathbf{R}^3$

In this work, we describe the baryon as the four-dimensional chiral soliton, i.e., the Skyrmion in holographic QCD. To see the validity of this approach for the baryon, we now compare the meson effective action induced by holographic QCD with that in a chiral perturbation theory (ChPT) as a low-energy effective theory of QCD [44]. The ChPT is phenomenologically constructed respecting the symmetry of QCD, the chiral symmetry and the Lorentz invariance in the four-dimensional space-time. With these symmetry constraints, there are three possible terms as the four-derivative terms of pion fields:

$$\text{tr}[L_\mu, L_\nu]^2, \quad \text{tr}\{L_\mu, L_\nu\}^2, \quad \text{tr}(\partial_\mu L_\nu)^2, \quad (34)$$

where  $L_\mu = \frac{1}{i}U^\dagger \partial_\mu U$  is the 1-form pion fields in Eq. (21). The first term  $\text{tr}[L_\mu, L_\nu]^2$ , called the ‘‘Skyrme term’’ [45], is to give the stability of the Skyrme soliton solution with finite size in the coordinate space. On the other hand, the other two terms are known to give the instability of Skyrme solitons [46]. The symmetry constraints in the ChPT cannot determine which terms should appear because all the terms in (34) are chiral symmetric and Lorentz invariant. Therefore Skyrme deliberately takes only the first term  $\text{tr}[L_\mu, L_\nu]^2$  in the meson effective action as an effective ‘‘model’’ for the baryon as the chiral soliton, which was called the ‘‘Skyrme model’’ [45].

Now, by starting from the holographic QCD with the five-dimensional Yang-Mills action (2) of the probe D8 brane, one can find only the Skyrme term without the other two in (34), which is manifestly seen in the action (20). Actually the five-dimensional Yang-Mills action (2) with  $O(F^2)$  includes two time derivatives at most, so that the appearances of the other two terms:  $\text{tr}\{L_\mu, L_\nu\}^2$  and  $\text{tr}(\partial_\mu L_\nu)^2$  with four time derivatives are forbidden at the leading order of  $1/N_c$  and  $1/\lambda$  expansion in holographic QCD. These comparisons with the chiral perturbation theory clearly indicate that holographic QCD is not just the low-energy effective theory of QCD only with the constraint of symmetries in four-dimensional space-time: ac-

tually, it obeys the  $U(N_f)$  symmetry extending to the extra fifth dimension  $z$ . Furthermore, one can see that the chiral soliton picture for the baryon is now supported by the holographic approach, retaining the direct connection with QCD. With these considerations, we employ the concept of chiral soliton picture for the baryon analysis in holographic QCD [9].

Now we begin with the hedgehog Ansatz for pion field  $U(\mathbf{x})$  and  $\rho$  meson field  $\rho_\mu(\mathbf{x})$  as a baryon configuration [9]:

$$U^*(\mathbf{x}) = e^{i\tau_a \hat{x}_a F(r)}, \quad \left( \hat{x}_a \equiv \frac{x_a}{r}, r \equiv |\mathbf{x}| \right) \quad (35)$$

$$\rho_0^*(\mathbf{x}) = 0, \quad \rho_i^*(\mathbf{x}) = \rho_{ia}^*(\mathbf{x}) \frac{\tau_a}{2} = \{\varepsilon_{iab} \hat{x}_b \tilde{G}(r)\} \tau_a, \quad (36)$$

$$(\tilde{G}(r) \equiv G(r)/r)$$

where  $\tau_a$  is the Pauli matrix, and  $F(r)$  is a dimensionless profile function of the pion field with boundary conditions  $F(0) = \pi$  and  $F(\infty) = 0$ , giving topological charge equal to unity. Ansatz (35) means  $\pi_a(\mathbf{x}) = \hat{x}_a F(r)$  for the pion field.  $G(r)$  is also a dimensionless profile function of the  $\rho$  meson field. This Ansatz for the  $\rho$  meson field is also called ‘‘Wu-Yang-’tHooft-Polyakov Ansatz’’ [47], and the same configuration Ansatz can be seen for the gauge field of the ’tHooft-Polyakov monopole [48].

By substituting the configuration Ansatz (35) and (36) into the four-dimensional meson effective action  $S_{\text{eff}}$  in (20) with the Euclidean metric, we can get the static hedgehog mass of a brane-induced Skyrmion on the flat space  $\mathbf{R}^3$  as follows (detailed derivations can be found in our previous paper [9]):

$$E[F(r), G(r)] \equiv [S_{\text{D8}}^{\text{DBI}} - S_{\text{D8}}^{\text{DBI}}|_{A_M \rightarrow 0}]_{\text{hedgehog}} \equiv \int_0^\infty 4\pi dr r^2 \cdot \varepsilon[F(r), G(r)], \quad (37)$$

$$\begin{aligned} r^2 \cdot \varepsilon[F(r), G(r)] &= \frac{f_\pi^2}{4} [2(r^2 F'^2 + 2\sin^2 F)] + m_\rho^2 [4r^2 \tilde{G}^2] + \frac{1}{32e^2} \left[ 16\sin^2 F \left( 2F'^2 + \frac{\sin^2 F}{r^2} \right) \right] \\ &+ \frac{1}{2} [8\{3\tilde{G}^2 + 2r\tilde{G}(\tilde{G}') + r^2 \tilde{G}'^2\}] - g_{3\rho} [16r\tilde{G}^3] + \frac{1}{2} g_{4\rho} [16r^2 \tilde{G}^4] \\ &+ g_1 [16\{F' \sin F \cdot (\tilde{G} + r\tilde{G}') + \sin^2 F \cdot \tilde{G}/r\}] - g_2 [16\sin^2 F \cdot \tilde{G}^2] - g_3 [16\sin^2 F \cdot (1 - \cos F)\tilde{G}/r] \\ &- g_4 [16(1 - \cos F)\tilde{G}^2] + g_5 [16r(1 - \cos F)\tilde{G}^3] + g_6 [16r^2 F'^2 \tilde{G}^2] + g_7 [8(1 - \cos F)^2 \tilde{G}^2], \quad (38) \end{aligned}$$

where  $F' \equiv \frac{dF(r)}{dr}$  ( $= \frac{\partial F(r)}{\partial r}$ ) and  $\tilde{G}' \equiv \frac{d\tilde{G}(r)}{dr}$  ( $= \frac{\partial \tilde{G}(r)}{\partial r}$ ).

Now we take the ‘‘Adkins-Nappi-Witten (ANW) unit’’ for energy and length as  $E_{\text{ANW}} \equiv \frac{f_\pi}{2e}$  and  $r_{\text{ANW}} \equiv \frac{1}{ef_\pi}$  [25], and we rewrite all variables in this ANW unit as  $\bar{E} \equiv \frac{1}{E_{\text{ANW}}} E$  and  $\bar{r} \equiv \frac{1}{r_{\text{ANW}}} r$ . By taking this scaled unit, the hedgehog energy density (38) of the single brane-induced Skyrmion on  $\mathbf{R}^3$  can be rewritten as follows (overlines of  $\bar{E}$  and  $\bar{r}$  below are abbreviated for simplicity):

$$\begin{aligned}
r^2 \cdot \varepsilon[F(r), G(r)] &= (r^2 F'^2 + 2\sin^2 F) + 2\left(\frac{m_\rho}{f_\pi}\right)^2 [4r^2 \tilde{G}^2] + \sin^2 F \left(2F'^2 + \frac{\sin^2 F}{r^2}\right) \\
&+ (2e^2) \frac{1}{2} [8\{3\tilde{G}^2 + 2r\tilde{G}(\tilde{G}') + r^2 \tilde{G}'^2\}] - (2e^2) g_{3\rho} [16r\tilde{G}^3] + (2e^2) \frac{1}{2} g_{4\rho} [16r^2 \tilde{G}^4] \\
&+ (2e^2) g_1 [16\{F' \sin F \cdot (\tilde{G} + r\tilde{G}') + \sin^2 F \cdot \tilde{G}/r\}] - (2e^2) g_2 [16\sin^2 F \cdot \tilde{G}^2] \\
&- (2e^2) g_3 [16\sin^2 F \cdot (1 - \cos F)\tilde{G}/r] - (2e^2) g_4 [16(1 - \cos F)\tilde{G}^2] + (2e^2) g_5 [16r(1 - \cos F)\tilde{G}^3] \\
&+ (2e^2) g_6 [16r^2 F'^2 \tilde{G}^2] + (2e^2) g_7 [8(1 - \cos F)^2 \tilde{G}^2]. \tag{39}
\end{aligned}$$

Here we comment about a scaling property of the brane-induced Skyrmion. The holographic QCD has just two parameters:  $\kappa (= \frac{\lambda N_c}{216\pi^3})$  and  $M_{\text{KK}}$ , so that the pion decay constant  $f_\pi$ , the  $\rho$  meson mass  $m_\rho$ , and the Skyrme parameter  $e$  in Eqs. (22)–(24) can be explicitly written by  $\kappa$  and  $M_{\text{KK}}$  in holographic QCD as

$$f_\pi = 2\sqrt{\frac{\kappa}{\pi}} M_{\text{KK}}, \tag{40}$$

$$m_\rho = \sqrt{\lambda_1} M_{\text{KK}} \simeq \sqrt{0.67} M_{\text{KK}}, \tag{41}$$

$$e = \frac{1}{4} \left[ \kappa \int dz K^{-1/3} \psi_+^2 (1 - \psi_+)^2 \right]^{-1/2} \simeq \frac{1}{4\sqrt{0.157}} \frac{1}{\sqrt{\kappa}}, \tag{42}$$

where the energy unit  $M_{\text{KK}}$  is recovered. By using these relations (40)–(42), the ANW unit for energy and length, i.e.,  $E_{\text{ANW}}$  and  $r_{\text{ANW}}$  can be written by  $\kappa$  and  $M_{\text{KK}}$  as

$$E_{\text{ANW}} = \frac{f_\pi}{2e} = \text{const} \cdot \kappa M_{\text{KK}}, \tag{43}$$

$$r_{\text{ANW}} = \frac{1}{ef_\pi} = \text{const} \cdot \frac{1}{M_{\text{KK}}}. \tag{44}$$

The five-dimensional Yang-Mills action (2) with  $O(F^2)$  is proportional to  $\kappa (= \frac{\lambda N_c}{216\pi^3})$ , as the leading order of  $1/N_c$  and  $1/\lambda$  expansion. Furthermore,  $M_{\text{KK}}$  is the sole energy scale of the holographic approach. Therefore, in the energy unit  $E_{\text{ANW}} (\propto \kappa M_{\text{KK}})$ , the total energy appears as a scale invariant variable. In fact, by introducing the rescaled  $\rho$  meson field  $\hat{G}(r)$  as

$$\hat{G}(r) \equiv \frac{1}{\sqrt{\kappa}} \tilde{G}(r), \tag{45}$$

and considering the  $\kappa$ -dependence of the basis  $\psi_1$  as  $\psi_1 \propto \frac{1}{\sqrt{\kappa}}$  in the normalization condition (13), one can analytically show that every energy density in each term of Eq. (39) and meson field configurations  $F(r)$  and  $\hat{G}(r)$  are scale invariant variables, being independent of the holographic two parameters,  $\kappa$  and  $M_{\text{KK}}$ .

With the considerations above, we give most discussions below in the ANW unit as the universal features of baryonic matter in holographic QCD, being independent of the definite values of  $f_\pi$  and  $m_\rho$ . The recovering of the

physical unit with the experimental inputs for  $f_\pi$  and  $m_\rho$  is discussed in Sec. VI, with respect to the critical densities of the phase transitions in the baryonic matter within the holographic approach.

### B. Brane-induced Skyrmion on $S^3$

Now we study the baryonic matter in holographic QCD by analyzing the system of single brane-induced Skyrmion on a three-dimensional closed manifold  $S^3$ .

In this study, we consider the baryonic matter with large  $N_c$  because holographic QCD is the large  $N_c$  effective theory, derived from the classical supergravity justified in the large  $N_c$  and large 'tHooft coupling [49]. According to the general analysis of large- $N_c$  QCD, a baryon mass is found to become  $O(N_c)$  [8,50], so that its kinetic energy becomes  $O(N_c^{-1})$ . As for the quantum effects of the baryonic matter, zero point quantum fluctuation energy  $E_0$  and baryon mass splitting  $\Delta m$  in the isospin projection correspond to the higher-order effects of  $1/N_c$  expansion:  $E_0 \sim O(N_c^0)$  and  $\Delta m \sim O(N_c^{-1})$  [25]. Therefore, with large- $N_c$  condition, we can consider that the kinetic energy and quantum effects are suppressed relative to the static mass, and the baryonic matter comes into the ‘‘static Skyrme matter.’’

Such static Skyrme matter was first analyzed by Klebanov [26], placing Skyrme soliton configurations periodically along the three-dimensional cubic lattice, which could be related with ‘‘nuclear crystal’’ with pion condensation in the deep interior of neutron stars. Therefore, by analyzing the static Skyrme matter, one can see some typical features of baryonic matter with large- $N_c$  conditions.

In this paper, we take certain mathematical tricks to analyze such static Skyrme matter suggested by Manton and Ruback [27]. To analyze the features of the multi-Skyrmion system on the flat coordinate space  $\mathbf{R}^3$ , they alternately treat the system of a single Skyrmion on a three-dimensional closed manifold  $S^3$  with finite radius  $R$  as shown in Fig. 1. Actually, the multi-Skyrmion system on  $\mathbf{R}^3$  and the system of a single Skyrmion on  $S^3$  can be related with each other through the compactification of the boundary for a unit cell on  $\mathbf{R}^3$  shared by the single Skyrmion as in Fig. 1. The interaction between the baryons in the medium on  $\mathbf{R}^3$  is simulated by the curvature of the closed manifold  $S^3$ . The baryon-number density can be

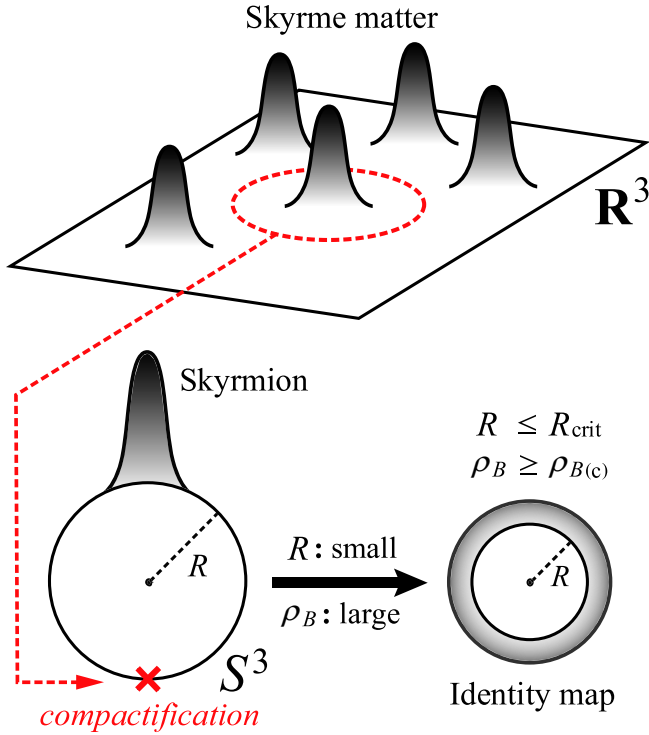


FIG. 1 (color online). Schematic figure of the static Skyrme matter on a flat coordinate space  $\mathbf{R}^3$ , and the system of a single Skyrmion on a closed manifold  $S^3$  with finite radius  $R$ . The static Skyrme matter on  $\mathbf{R}^3$  and the system of a single Skyrmion on  $S^3$  can be related with each other through the compactification of the boundary for a unit cell on  $\mathbf{R}^3$  shared by the single Skyrmion. The decrease of the radius  $R$  of  $S^3$  represents the increase of the baryon-number density  $\rho_B (\equiv (2\pi^2 R^3)^{-1})$  in the medium in this modeling. For  $R \leq R_{\text{crit}}$  as a critical radius, i.e.,  $\rho_B \geq \rho_{B(c)} (\equiv \{2\pi^2 (R_{\text{crit}})^3\}^{-1})$  as a critical density, the energy density of the single Skyrmion becomes uniform distribution as the “identity map” discussed in Eq. (67), which is called the “delocalization phase transition.”

represented as  $\rho_B = 1/2\pi^2 R^3$  on  $S^3$ , so that as the size of  $S^3$  decreases, the increase of the baryon-number density in the medium is represented in this modeling. Actually, as the radius  $R$  of  $S^3$  decreases, the energy density of a single baryon is found to delocalize due to the medium effects in the baryonic matter [27], and, below the critical radius  $R_{\text{crit}}$  of  $S^3$ , the energy density of the baryon coincides with the uniform distribution as the “identity map,” which is called the “delocalization phase transition” shown in Fig. 1. Such delocalization phase transition in the Skyrme model can be related with the deconfinement of the baryon and also the chiral symmetry restoration in QCD, which will be inclusively discussed by taking the order parameters in Sec. V. With these considerations, by analyzing the system of a single brane-induced Skyrmion on  $S^3$ , we can see some typical features of baryonic matter in holographic QCD. Especially, by comparing the standard Skyrmion without  $\rho$  mesons and the brane-induced Skyrmion on  $S^3$ , the roles of (axial) vector mesons in the high density phase of baryonic

matter can be discussed from the holographic point of view.

Now we introduce the projection procedure from the flat space  $\mathbf{R}^3$  onto the curved space  $S^3$  [51], to get a hedgehog mass of a brane-induced Skyrmion on  $S^3$ . First, we consider the three-dimensional orthogonal space  $\mathbf{R}^3$  in polar coordinates as

$$\begin{aligned} \mathbf{x} &= (z, x, y) = (r \cos\theta, r \sin\theta \cos\phi, r \sin\theta \sin\phi) \\ &= (r, \theta, \phi)_{3 \text{ dim.polar}} \end{aligned} \quad (46)$$

The integral operator  $d\hat{\mathbf{x}}$  and the derivation  $d$  can be written in polar coordinates as

$$d\hat{\mathbf{x}} = (d\hat{r}, d\hat{\theta}, d\hat{\phi})_{3 \text{ dim.polar}} = (dr, r d\theta, r \sin\theta d\phi)_{3 \text{ dim.polar}} \quad (47)$$

$$\begin{aligned} d &= dr \frac{\partial}{\partial r} + d\theta \frac{\partial}{\partial \theta} + d\phi \frac{\partial}{\partial \phi} \\ &= d\hat{r} \frac{\partial}{\partial r} + d\hat{\theta} \frac{1}{r} \frac{\partial}{\partial \theta} + d\hat{\phi} \frac{1}{r \sin\theta} \frac{\partial}{\partial \phi}, \end{aligned} \quad (48)$$

so that the differential operator  $\partial$  can be written as

$$\partial = \left( \frac{\partial}{\partial r}, \frac{1}{r} \frac{\partial}{\partial \theta}, \frac{1}{r \sin\theta} \frac{\partial}{\partial \phi} \right)_{3 \text{ dim.polar}}. \quad (49)$$

Second, we consider the four-dimensional orthogonal space  $\mathbf{R}^4$  in polar coordinates as

$$\begin{aligned} \mathbf{X} &= (t, z, x, y) \\ &= (R \cos\Theta, R \sin\Theta \cos\theta, R \sin\Theta \sin\theta \cos\phi, \\ &\quad R \sin\Theta \sin\theta \sin\phi) \\ &= (R, \Theta, \theta, \phi)_{4 \text{ dim.polar}} \end{aligned} \quad (50)$$

The integral operator  $d\hat{\mathbf{x}}$  and the derivation  $d$  can be written in polar coordinates as

$$\begin{aligned} d\hat{\mathbf{x}} &= (d\hat{R}, d\hat{\Theta}, d\hat{\theta}, d\hat{\phi})_{4 \text{ dim.polar}} \\ &= (dR, R d\Theta, R \sin\Theta d\theta, R \sin\Theta \sin\theta d\phi)_{4 \text{ dim.polar}} \end{aligned} \quad (51)$$

$$\begin{aligned} d &= dR \frac{\partial}{\partial R} + d\Theta \frac{\partial}{\partial \Theta} + d\theta \frac{\partial}{\partial \theta} + d\phi \frac{\partial}{\partial \phi} \\ &= d\hat{R} \frac{\partial}{\partial R} + d\hat{\Theta} \frac{1}{R} \frac{\partial}{\partial \Theta} + d\hat{\theta} \frac{1}{R \sin\Theta} \frac{\partial}{\partial \theta} \\ &\quad + d\hat{\phi} \frac{1}{R \sin\Theta \sin\theta} \frac{\partial}{\partial \phi}, \end{aligned} \quad (52)$$

so that the differential operator  $\partial$  can be written as

$$\partial = \left( \frac{\partial}{\partial R}, \frac{1}{R} \frac{\partial}{\partial \Theta}, \frac{1}{R \sin\Theta} \frac{\partial}{\partial \theta}, \frac{1}{R \sin\Theta \sin\theta} \frac{\partial}{\partial \phi} \right)_{4 \text{ dim.polar}}. \quad (53)$$

Now, by limiting the four-dimensional orthogonal space  $\mathbf{R}^4$  onto the surface of a three-dimensional closed manifold  $S^3$  with fixed radius  $R$ , the coordinate  $t$  in Eq. (50) becomes dependent on the other coordinates  $(z, x, y)$ . Furthermore,  $dR$  and  $\frac{\partial}{\partial R}$  can be regarded as zero in Eqs. (51) and (53) because the radial coordinate  $R$  is fixed on  $S^3$ . Therefore, by comparing Eqs. (46), (47), and (49) on  $\mathbf{R}^3$ , and Eqs. (50), (51), and (53) on  $S^3$  with fixed radius  $R$ , we find the projection procedure from  $\mathbf{R}^3$  to  $S^3$  as follows:

$$r \rightarrow R \sin\Theta, \quad (54)$$

$$dr \rightarrow R d\Theta, \quad (55)$$

$$\frac{\partial}{\partial r} \rightarrow \frac{1}{R} \frac{\partial}{\partial \Theta}. \quad (56)$$

Recall that the hedgehog mass on  $\mathbf{R}^3$  with energy density in Eq. (39) can be written with its explicit arguments for the energy density as

$$E = \int_0^\infty 4\pi dr r^2 \cdot \varepsilon \left[ F(r), G(r), \frac{\partial}{\partial r} F(r), \frac{\partial}{\partial r} G(r), r \right]. \quad (57)$$

By applying the projection procedure (54)–(56) to the hedgehog mass on  $\mathbf{R}^3$  in Eq. (57), we can get the hedgehog mass on  $S^3$  as

$$\begin{aligned} E &= \int_0^\pi 4\pi R d\Theta R^2 \sin^2\Theta \cdot \varepsilon \left[ F(R \sin\Theta), G(R \sin\Theta), \right. \\ &\quad \left. \frac{1}{R} \frac{\partial}{\partial \Theta} F(R \sin\Theta), \frac{1}{R} \frac{\partial}{\partial \Theta} G(R \sin\Theta), R \sin\Theta \right] \quad (58) \\ &= \int_0^{\pi R} 4\pi dr R^2 \sin^2 \frac{r}{R} \\ &\quad \cdot \varepsilon \left[ F(r), G(r), \frac{\partial}{\partial r} F(r), \frac{\partial}{\partial r} G(r), R \sin \frac{r}{R} \right]. \quad (59) \end{aligned}$$

In Eq. (59), we introduce a new variable  $r$  as the arc length on  $S^3$  as

$$r \equiv R\Theta, \quad (60)$$

and  $r$ -dependent dimensionless functions  $F(R \sin \frac{r}{R})$  and  $G(R \sin \frac{r}{R})$  are renamed again as  $F(r)$  and  $G(r)$ . Therefore, by comparing Eq. (57) on  $\mathbf{R}^3$  and Eq. (59) on  $S^3$ , we can get the simple projection procedure for the hedgehog energy density from  $\mathbf{R}^3$  to  $S^3$  as

$$\begin{aligned} dr r^2 \cdot \varepsilon \left[ F(r), G(r), \frac{\partial}{\partial r} F(r), \frac{\partial}{\partial r} G(r), r \right] \\ \rightarrow dr R^2 \sin^2 \frac{r}{R} \cdot \varepsilon \left[ F(r), G(r), \frac{\partial}{\partial r} F(r), \frac{\partial}{\partial r} G(r), R \sin \frac{r}{R} \right], \quad (61) \end{aligned}$$

where the topological boundary for the chiral field  $F(r)$  in (35) is also projected on  $S^3$  as

$$F(0) = \pi, \quad F(\pi R) = 0. \quad (62)$$

Now, by applying the projection procedure (61) for the hedgehog energy density on  $\mathbf{R}^3$  in Eq. (39), we can eventually get the hedgehog energy density on  $S^3$  with ANW units as follows (Note here that the dimensional profile function  $\tilde{G}(r) = G(r)/r$  on  $\mathbf{R}^3$  is to be naturally introduced on  $S^3$  through the projection procedure as  $\tilde{G}(r) \equiv \frac{G(r)}{R \sin \frac{r}{R}}$ ):

$$E[F(r), G(r)] = \int_0^{\pi R} 4\pi dr R^2 \sin^2 \frac{r}{R} \cdot \varepsilon[F(r), G(r)], \quad (63)$$

$$\begin{aligned} R^2 \sin^2 \frac{r}{R} \cdot \varepsilon[F(r), G(r)] &= \left( R^2 \sin^2 \frac{r}{R} \cdot F'^2 + 2 \sin^2 F \right) + 2 \left( \frac{m_\rho}{f_\pi} \right)^2 \left[ 4 R^2 \sin^2 \frac{r}{R} \cdot \tilde{G}^2 \right] + \sin^2 F \left( 2 F'^2 + \frac{\sin^2 F}{R^2 \sin^2 \frac{r}{R}} \right) \\ &\quad + (2e^2) \frac{1}{2} \left[ 8 \left\{ \left( 2 + \cos^2 \frac{r}{R} \right) \tilde{G}^2 + 2 R \sin \frac{r}{R} \cos \frac{r}{R} \cdot \tilde{G}(\tilde{G}') + R^2 \sin^2 \frac{r}{R} \cdot \tilde{G}'^2 \right\} \right] \\ &\quad - (2e^2) g_{3\rho} \left[ 16 R \sin \frac{r}{R} \cdot \tilde{G}^3 \right] + (2e^2) \frac{1}{2} g_{4\rho} \left[ 16 R^2 \sin^2 \frac{r}{R} \cdot \tilde{G}^4 \right] \\ &\quad + (2e^2) g_1 \left[ 16 \left\{ F' \sin F \cdot \left( \cos \frac{r}{R} \cdot \tilde{G} + R \sin \frac{r}{R} \cdot \tilde{G}' \right) + \sin^2 F \cdot \tilde{G} \left/ \left( R \sin \frac{r}{R} \right) \right. \right\} \right] \\ &\quad - (2e^2) g_2 \left[ 16 \sin^2 F \cdot \tilde{G}^2 \right] - (2e^2) g_3 \left[ 16 \sin^2 F \cdot (1 - \cos F) \tilde{G} \left/ \left( R \sin \frac{r}{R} \right) \right. \right] \\ &\quad - (2e^2) g_4 \left[ 16 (1 - \cos F) \tilde{G}^2 \right] + (2e^2) g_5 \left[ 16 R \sin \frac{r}{R} \cdot (1 - \cos F) \tilde{G}^3 \right] \\ &\quad + (2e^2) g_6 \left[ 16 R^2 \sin^2 \frac{r}{R} \cdot F'^2 \tilde{G}^2 \right] + (2e^2) g_7 \left[ 8 (1 - \cos F)^2 \tilde{G}^2 \right], \quad (64) \end{aligned}$$

where  $F' \equiv \frac{dF(r)}{dr} (= \frac{\partial F(r)}{\partial r})$  and  $\tilde{G}' \equiv \frac{d\tilde{G}(r)}{dr} (= \frac{\partial \tilde{G}(r)}{\partial r})$ . Here measures as  $R^2 \sin^2 \frac{r}{R}$  newly appear in the energy density (64) relative to Eq. (39) on the flat space  $\mathbf{R}^3$ , indicating the existence of the curvature of the closed manifold  $S^3$ . We also construct the Euler-Lagrange equations for the pion field  $F(r)$  and  $\rho$  meson field  $\tilde{G}(r)$  from the energy density in Eq. (64) as follows:

$$\begin{aligned} \frac{1}{4\pi} \left\{ \frac{\delta E}{\delta F(r)} - \frac{d}{dr} \left( \frac{\delta E}{\delta F'(r)} \right) \right\} = & \left( -4R \sin \frac{r}{R} \cos \frac{r}{R} \cdot F' - 2R^2 \sin^2 \frac{r}{R} \cdot F'' + 4 \sin F \cdot \cos F \right) \\ & + \left\{ -4 \sin F \cdot \cos F \cdot F'^2 - 4 \sin^2 F \cdot F'' + 4 \sin^3 F \cdot \cos F \right\} / \left( R^2 \sin^2 \frac{r}{R} \right) \\ & + (2e^2)g_1 \left[ 16 \left\{ 2 \sin F \cdot \cos F \cdot \tilde{G} \right\} / \left( R \sin \frac{r}{R} \right) \right. \\ & \left. - \sin F \cdot \left( -\frac{1}{R} \sin \frac{r}{R} \cdot \tilde{G} + 2 \cos \frac{r}{R} \cdot \tilde{G}' + R \sin \frac{r}{R} \cdot \tilde{G}'' \right) \right] - (2e^2)g_2 [16(2 \sin F \cdot \cos F \cdot \tilde{G}^2)] \\ & - (2e^2)g_3 \left[ 16(\sin F + 2 \sin F \cdot \cos F - 3 \sin F \cdot \cos^2 F) \tilde{G} \right] / \left( R \sin \frac{r}{R} \right) \\ & - (2e^2)g_4 [16(\sin F \cdot \tilde{G}^2)] + (2e^2)g_5 \left[ 16 \left( R \sin \frac{r}{R} \sin F \cdot \tilde{G}^3 \right) \right] \\ & + (2e^2)g_6 \left[ 16 \left( -4R \sin \frac{r}{R} \cos \frac{r}{R} \cdot F' \tilde{G}^2 - 2R^2 \sin^2 \frac{r}{R} \cdot F'' \tilde{G}^2 - 4R^2 \sin^2 \frac{r}{R} \cdot F' \tilde{G} \tilde{G}' \right) \right] \\ & + (2e^2)g_7 [8\{2(1 - \cos F) \sin F \cdot \tilde{G}^2\}] = 0, \end{aligned} \quad (65)$$

$$\begin{aligned} \frac{1}{4\pi} \left\{ \frac{\delta E}{\delta \tilde{G}(r)} - \frac{d}{dr} \left( \frac{\delta E}{\delta \tilde{G}'(r)} \right) \right\} = & 2 \left( \frac{m_\rho}{f_\pi} \right)^2 \left[ 4 \left( 2R^2 \sin^2 \frac{r}{R} \cdot \tilde{G} \right) \right] \\ & + (2e^2) \frac{1}{2} \left[ 8 \left( 4\tilde{G} + 2 \sin^2 \frac{r}{R} \cdot \tilde{G} - 4R \sin \frac{r}{R} \cos \frac{r}{R} \cdot \tilde{G}' - 2R^2 \sin^2 \frac{r}{R} \cdot \tilde{G}'' \right) \right] \\ & - (2e^2)g_{3\rho} \left[ 16 \left( 3R \sin \frac{r}{R} \cdot \tilde{G}^2 \right) \right] + (2e^2) \frac{1}{2} g_{4\rho} \left[ 16 \left( 4R^2 \sin^2 \frac{r}{R} \cdot \tilde{G}^3 \right) \right] \\ & + (2e^2)g_1 \left[ 16 \left\{ \sin^2 F \right\} / \left( R \sin \frac{r}{R} \right) - R \sin \frac{r}{R} \cos F \cdot F'^2 - R \sin \frac{r}{R} \sin F \cdot F'' \right] \\ & - (2e^2)g_2 [16(2 \sin^2 F \cdot \tilde{G})] - (2e^2)g_3 \left[ 16 \sin^2 F (1 - \cos F) \right] / \left( R \sin \frac{r}{R} \right) \\ & - (2e^2)g_4 \left[ 16 \left\{ 2(1 - \cos F) \tilde{G} \right\} \right] + (2e^2)g_5 \left[ 16 \left\{ 3R \sin \frac{r}{R} (1 - \cos F) \tilde{G}^2 \right\} \right] \\ & + (2e^2)g_6 \left[ 16 \left\{ 2R^2 \sin^2 \frac{r}{R} \cdot F'^2 \tilde{G} \right\} \right] + (2e^2)g_7 [8\{2(1 - \cos F)^2 \tilde{G}\}] = 0. \end{aligned} \quad (66)$$

Now one can show that the Euler-Lagrange equations (65) and (66) always have the analytical solution for arbitrary value of radius  $R$  of  $S^3$  as

$$F(r) = \pi - \frac{r}{R}, \quad \tilde{G}(r) = 0, \quad (67)$$

which is the ‘‘identity map’’ solution in the standard Skyrme model without  $\rho$  meson field [27]. In the Skyrme model, the energy density of the baryon is generated by the spatial gradient of the pion fields. Therefore, such linear configuration as in Eq. (67) gives the uniform energy distributions with its classical mass as

$$E_{\text{id}} = \left( R + \frac{1}{R} \right) 6\pi^2, \quad (68)$$

which can be given by substituting the linear configuration (67) into the energy density (64). Hence the change of the absolute minimum solution from the localized Skyrmion into the identity map (67) can be regarded as a signal of transitions from the localized phase to the uniform phase of the baryonic matter, referred to as the delocalization phase transition. Note that the identity map solution (67) has no  $\rho$  meson configuration:  $\tilde{G}(r) = 0$ . Therefore, if the identity map is realized as the absolute minimum solution, it indicates that  $\rho$  meson field absolutely disappears in the high

density phase, which is discussed with numerical results in Sec. IV.

#### IV. BARYON NATURE IN DENSE QCD

In this section, we show the numerical results and discussions about the baryon nature in dense QCD by solving the Euler-Lagrange equations (65) and (66) derived from holographic QCD. The energy density and the field configuration profiles of the baryon are analyzed in Sec. IV A. A new striking picture of ‘‘pion dominance’’ near the critical density is proposed in Sec. IV B. The mass and root-mean-square mass radius of the baryon are examined in Sec. IV C. We explain the swelling mechanism of the baryon in the general context of QCD in Sec. IV D. Through all of the sections below, by comparing the Skyrme model without  $\rho$  meson field and the brane-induced Skyrme (BIS) model on  $S^3$ , the roles of (axial) vector mesons in the baryonic matter are discussed from a holographic point of view.

##### A. Energy density and field configuration profiles

In this section, we discuss the baryon-number density dependence of the energy density and the field configuration profiles of a single baryon for the Skyrme model and the BIS model by changing the size of the manifold  $S^3$ . Actually, the baryon-number density is represented as  $\rho_B = 1/2\pi^2 R^3$  on  $S^3$ , so that, as the radius  $R$  of  $S^3$  decreases, the increase of total baryon-number density in the medium is represented in this modeling.

First, we show in Fig. 2 the energy density of the baryon for the Skyrme model with radius  $R$  of  $S^3$ . One can see that the energy density tends to delocalize as  $R$  decreases, which can be regarded as some medium effects in the dense baryonic matter. Below the critical radius,  $R \leq$

$R_{\text{crit}}^{\text{Skyrme}} = \sqrt{2}$ , the energy-density distribution of the baryon exactly coincides with the uniform one as the identity map denoted by the dashed lines in Fig. 2. The transition from localized energy density into uniform one is called the ‘‘delocalization phase transition.’’

Next we show in Fig. 3 the same plot in the case of the BIS model. The energy density of the baryon also tends to delocalize as  $R$  decreases. However, the delocalization along with the decrease of  $R$  is delayed relative to the Skyrme model without  $\rho$  meson field, and the energy distribution is still localized even around  $R \sim R_{\text{crit}}^{\text{Sky}} = \sqrt{2}$ , which is the critical radius for the Skyrme model. In fact, the heavy  $\rho$  meson field appearing in the core region of the baryon is to provide the attraction with the pion field, which leads to the shrinkage of the total size of the baryon [9]. Therefore, the smaller radius of  $S^3$ , i.e., the larger baryon-number density is needed for the BIS model to give the delocalization phase transition, which is discussed in Sec. VI with recovering the physical units. Then, below the critical radius,  $R \leq R_{\text{crit}}^{\text{BIS}} = 1.19$ , the energy density distribution of the baryon in the BIS model becomes the uniform one as identity map (67). These delocalization phase transitions in the Skyrmin picture can be related with the deconfinement of the baryon and also the chiral symmetry restoration, which will be discussed with the order parameters in Sec. V.

We can also show in Fig. 4 the comparison between the energy density of the baryon and  $\rho$  meson contributions in the interaction terms of the BIS model (64) for  $R = 4.0$ ,  $\sqrt{2}$ , and 1.19. For  $R = 4.0$  and  $\sqrt{2}$ , one can see the manifest contributions from the  $\rho$  meson field in the core region of the baryon. On the other hand, at the critical radius  $R = R_{\text{crit}}^{\text{BIS}} = 1.19$ , all the contributions from the  $\rho$  meson field absolutely disappear in the uniform phase.

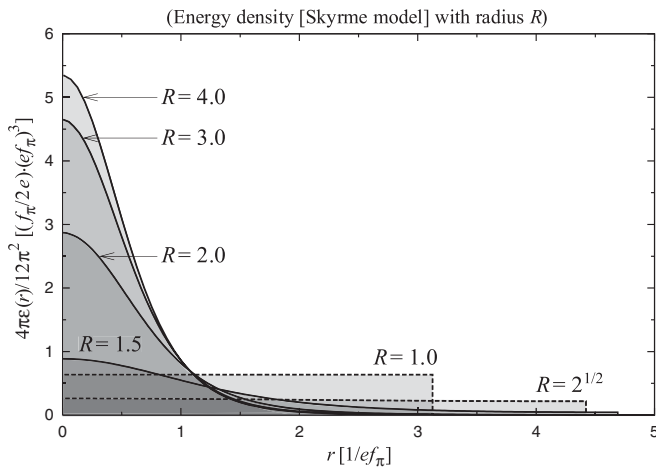


FIG. 2. Energy density of a single baryon for the Skyrme model with radius  $R$  of  $S^3$ . Below the critical radius,  $R \leq R_{\text{crit}}^{\text{Skyrme}} = \sqrt{2}$ , energy density becomes a uniform distribution as the identity map, shown by the dashed lines.

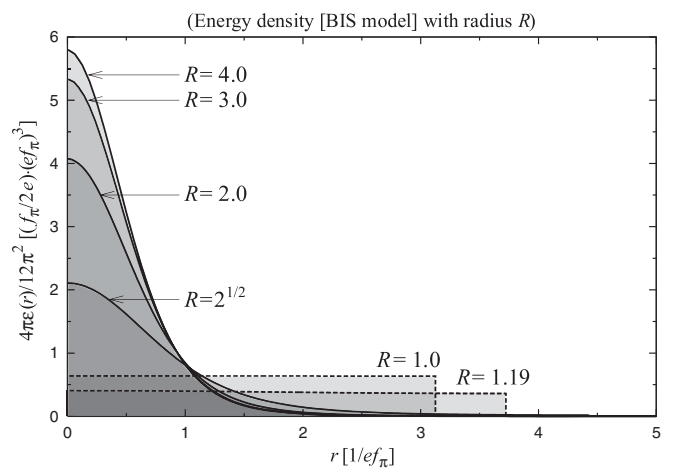


FIG. 3. Energy density of single baryon for the BIS model with radius  $R$  of  $S^3$ . Below the critical radius,  $R \leq R_{\text{crit}}^{\text{BIS}} = 1.19$ , energy density becomes a uniform distribution as the identity map, shown by the dashed lines.

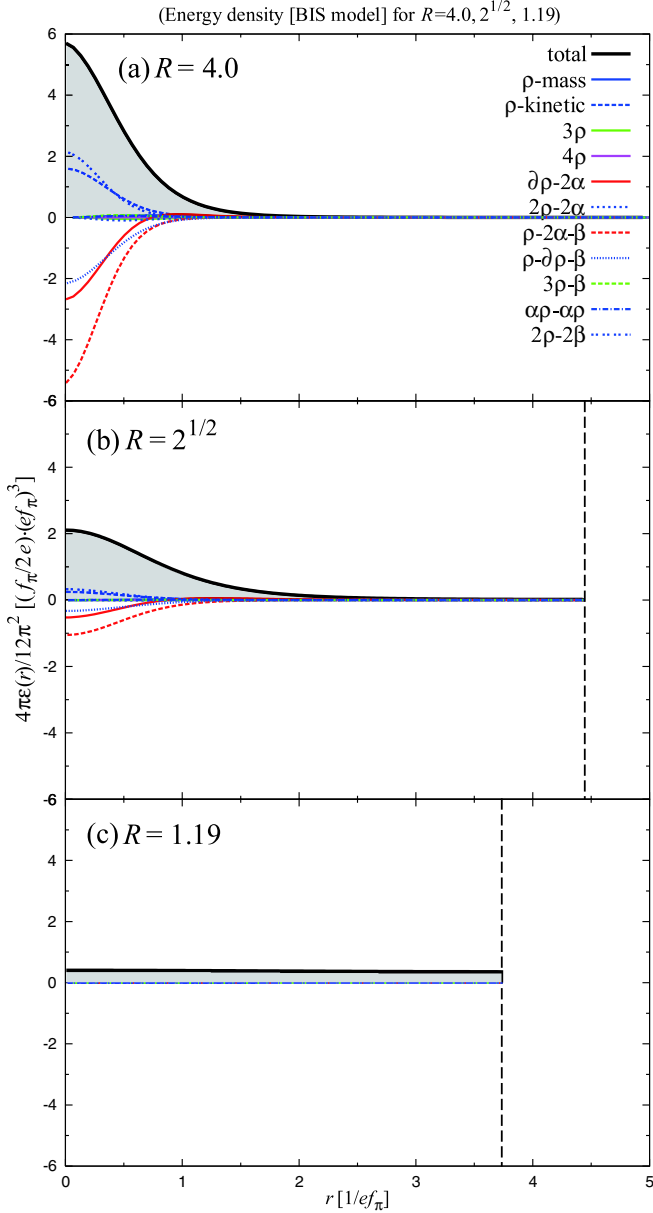


FIG. 4 (color online). Energy density of single baryon and  $\rho$  meson contributions in the terms of the BIS model (64) for  $R = 4.0, \sqrt{2}$ , and 1.19. Labels for lines in (a) denote each term in (64), e.g. “ $4\rho$ ” corresponds to  $(-1/2)g_{4\rho} \int d^4x \text{tr}[\rho_\mu, \rho_\nu]^2$  (See Ref. [9] for labels). The vertical dashed lines in (b) and (c) show the boundaries of  $S^3$  at the south pole  $r = \pi R$ , respectively. At the critical radius,  $R = R_{\text{crit}}^{\text{BIS}} = 1.19$  in (c), energy density becomes a uniform distribution as the identity map, where the  $\rho$  meson contributions disappear and only pion contribution survives as the “pion dominance.”

We also show the field configuration profiles of the pion and the  $\rho$  meson in Fig. 5 and 6, respectively, in the BIS model for  $R = 4.0, \sqrt{2}$ , and 1.19. As  $R$  decreases, the pion field  $F(r)$  in Fig. 5 approaches to the linear configuration as the identity map in Eq. (67), giving the uniform energy density distribution. As for the  $\rho$  meson field in Fig. 6,

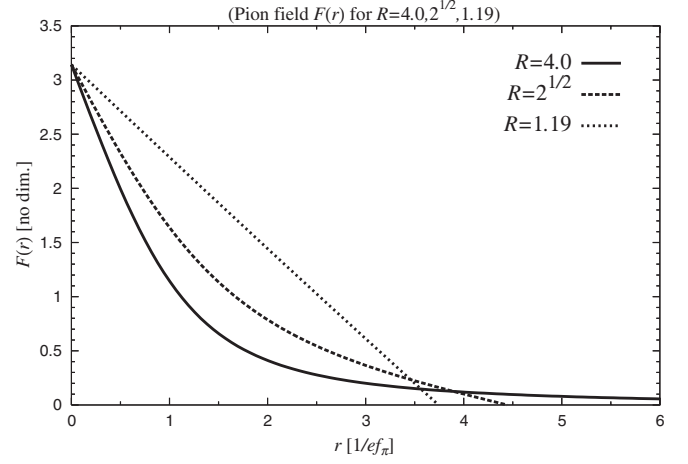


FIG. 5. Pion field  $F(r)$  of the BIS model for  $R = 4.0, \sqrt{2}$ , and 1.19. At the critical radius,  $R = R_{\text{crit}}^{\text{BIS}} = 1.19$ ,  $F(r)$  coincides with a linear configuration as the identity map in Eq. (67).

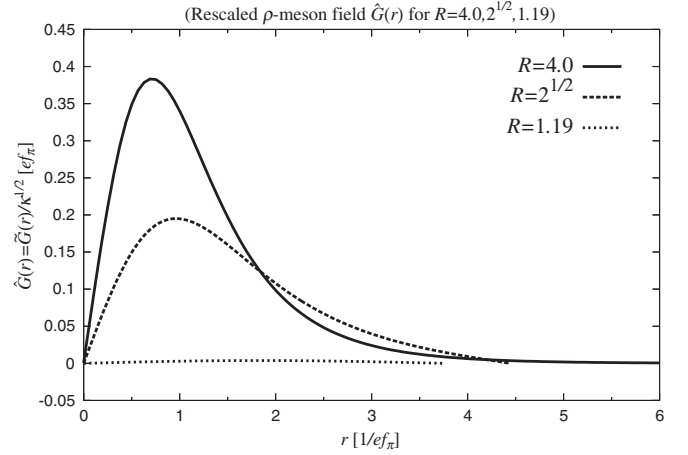


FIG. 6. Rescaled  $\rho$  meson field  $\hat{G}(r) = \frac{\tilde{G}(r)}{\sqrt{\kappa}}$  of the BIS model for  $R = 4.0, \sqrt{2}$ , and 1.19. At the critical radius,  $R = R_{\text{crit}}^{\text{BIS}} = 1.19$ ,  $\hat{G}(r)$  becomes zero configuration as the identity map in Eq. (67).

amplitude of  $\rho$  meson field  $\hat{G}(r)$  tends to decrease as  $R$  decreases, and it absolutely disappears below the critical radius,  $R \leq R_{\text{crit}}^{\text{BIS}} = 1.19$  as the identity map in Eq. (67). These results indicate that the amplitude of the  $\rho$  meson field decreases as the baryon-number density increases in the medium, and it absolutely disappears and only the pion field survives near the critical density.

## B. Pion dominance near critical density

In the previous section, we find that the  $\rho$  meson field would disappear near the critical density. Now we propose a conjecture that such disappearance of the  $\rho$  meson field near the critical density can be generalized to all the other (axial) vector meson fields:  $a_1, \rho', a_1', \rho'' \dots$ , denoted by

the field  $B_\mu^{(n)}(x_\nu)$  in Eq. (7) by the following reasons within the holographic approach:

- (1) The kinetic term of (axial) vector meson field  $B_\mu^{(n)}$  on the closed manifold  $S^3$  is proportional to  $R^{-2}$  as

$$\text{tr}\{\partial_\mu B_\nu^{(n)} - \partial_\nu B_\mu^{(n)}\}^2 \propto R^{-2}, \quad (69)$$

which can be derived from a simple dimensional analysis. In general, the kinetic energy indicates the “kink” energy of field configurations. Therefore, the kinetic energy in Eq. (69) suppresses the spatial dependence of the field configuration  $B_\mu^{(n)}$  for small  $R$ , i.e., for the high density state, giving flat configuration in the high density phase.

- (2) The mass term  $m_n^2 \text{tr}\{B_\mu^{(n)} B_\mu^{(n)}\}$  suppresses the absolute value of  $B_\mu^{(n)}$  field more severely in accordance with its larger mass  $m_n^2$ .
- (3) The couplings between pions and heavier (axial) vector mesons  $B_\mu^{(n)}$  with larger index  $n$  are found to become smaller, which is suggested by the “bottom-up” dimensional deconstruction model [31] and also the “top-down” holographic approach [9]. In fact, within the holographic models, the origin of the meson mass in four-dimensional space-time can be regarded as the oscillation of the meson wave function in the extra fifth dimension  $z$ , denoted by the mass relation  $m_n^2 = \lambda_n$  in Sec. II. Such larger oscillations of heavier (axial) vector mesons wave functions in the fifth dimension have the smaller overlap with that of pions, giving the smaller coupling constants with pions in four-dimensional space-time [9]. In fact, some recent experiments with the hadron reactions provide some interesting data, showing that the heavier (axial) vector mesons tend to have smaller width for the decay into pions despite of larger phase space [52], which may be consistent with the prediction of holographic QCD as their smaller coupling constants with pions as mentioned above. Hence the effects of heavier (axial) vector mesons should be smaller for a baryon as a large-amplitude pion field, i.e., the chiral soliton.

These considerations (1), (2), (3) about the meson effective action in holographic QCD should support our conjecture about the general disappearance of (axial) vector meson fields in the high density phase. In other words, *only the pion fields survive near the critical density in the large- $N_c$  baryonic matter*. We call this phenomenon “pion dominance” near the critical density.

In Sec. VI, we will show that, even if the  $\rho$  meson field disappears near the critical point, it affects the critical density of the phase transition through its mass and also the interactions with the pion field in the action  $S_{\text{eff}}$  in Eq. (19). In this sense, even with the pion dominance near

the critical point proposed above, the (axial) vector mesons may still affect the critical phenomena like the critical density through their contributions in the effective action if they are included.

As for the survival of the pion fields near the critical density as the pion dominance, we give the following reason: the unit baryon-number on the manifold  $S^3$  comes from the boundary conditions of the pion hedgehog configuration  $F(r)$  at the north ( $r = 0$ ) and the south ( $r = \pi R$ ) poles on  $S^3$  as  $F(0) = \pi$  and  $F(\pi R) = 0$  in (62). In this sense, pions play the essential roles for the baryon-number current with their field boundaries. Therefore, the pion field cannot disappear because of the baryon-number constraint (62) for each unit cell of the manifold  $S^3$ . On the other hand, there is no constraints for the other (axial) vector meson fields, and they can disappear in the high density phase as some representation of “deconfinement.”

Such dominance of the pion field near the transition point might be somehow related with the appearance of chiral plasma modes  $\pi$  and  $\sigma$  above  $T_c$  of the deconfinement phase transition observed in the lattice QCD study [53]. In fact, the screening masses were measured for a variety of color-singlet channels with the quantum number of  $\pi$ ,  $\sigma$ ,  $\rho$ ,  $b_1$ , and  $a_1$  mesons. The chiral multiplet of  $\pi$  and  $\sigma$  was found to appear as the bound state even above  $T_c$ , whereas the other (axial) vector mesons would be in the continuum with the threshold as the twice of the lowest Matsubara frequency, i.e.,  $2\pi T$ . Such survival of the chiral plasma modes above  $T_c$  would inspire the concept of the strong-coupling quark-gluon plasma (sQGP) due to the long-range, nonperturbative effects of the strong interaction even at the highest temperature, instead of the naive free gas picture of quarks and gluons only due to the asymptotic freedom. Such strong correlation would also develop even at a dense regime of QCD, which may give some linking of our analysis with “pion dominance” in dense QCD.

By seeing some QCD phenomenologies, one can also find that quark degrees of freedom are often represented by “pions.” For example, in the case of the chiral quark model [54,55], quark–antiquark correlations are represented by pionic collective modes through the bosonization scheme for QCD, giving the “Cheshire cat picture” where the quark dynamics are represented by pions. In fact, it has provided a foundation of a Skyrme soliton picture for the baryon as a large-amplitude pion field. These traditional phenomenologies may also support the dominance of the pions near the critical density in the baryonic matter, with the appearance of quark-gluon dynamics.

### C. Mass and root-mean-square mass radius

In this section, we discuss the baryon-number density dependence of the mass and the root-mean-square (RMS) mass radius of a single baryon for the Skyrme model and the BIS model, by changing the size of the manifold  $S^3$ .

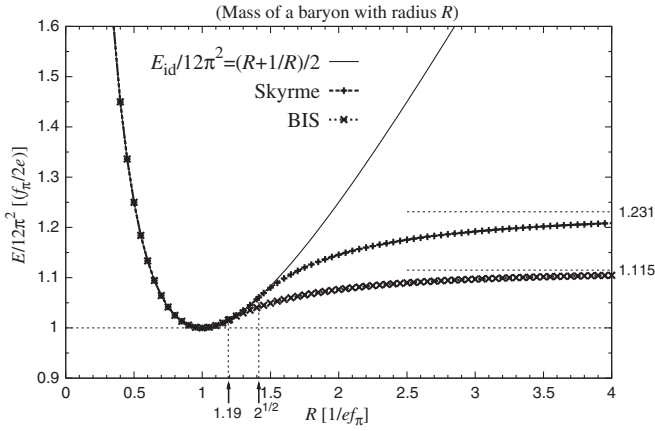


FIG. 7. Mass of a single baryon for the identity map, the Skyrme model, and the BIS model with radius  $R$  of  $S^3$ . The variables “1.231” and “1.115” are the masses of the baryon on the flat space  $\mathbf{R}^3$  for the Skyrme model and the BIS model, respectively.

In Fig. 7, we show the mass of the baryon for the Skyrme model and the BIS model with radius  $R$  of  $S^3$ . In the case of the Skyrme model, the mass decreases from the value on the flat space  $\mathbf{R}^3$ :  $1.231 \times 12\pi^2 [\frac{f_\pi}{2e}]$  [45] as  $R$  decreases, and it coincides with the mass of the identity map below the critical radius,  $R \leq R_{\text{crit}}^{\text{Skyrme}} = \sqrt{2}$  [27]. This coincidence of the numerical solution with the identity map indicates the transition from the localized phase to the uniform phase as the delocalization phase transition. In the case of the BIS model, the mass decreases from the value on  $\mathbf{R}^3$ :  $1.115 \times 12\pi^2 [\frac{f_\pi}{2e}]$  [9] as  $R$  decreases, and it coincides with the mass of the identity map below the critical radius,  $R \leq R_{\text{crit}}^{\text{BIS}} = 1.19$ , which is smaller than  $R_{\text{crit}}^{\text{Skyrme}}$  due to the shrinkage of the baryon by the  $\rho$  meson effects.

From a physical point of view, the decrease of the baryon mass as  $R$  decreases in Fig. 7 might come from the partial restoration of chiral symmetry in the dense baryonic matter, which will be discussed with the order parameter in Sec. V. This result is related with the well-known picture of the baryon mass generation from the quark condensate in the vacuum, suggested in some QCD phenomenologies, e.g., the QCD sum rules with the Ioffe formula [56], and also other chiral effective models [57,58]. In fact, the decrease of the baryon mass with the chiral symmetry restoration is observed in the finite-temperature lattice QCD study [42]. Note also that the decrease of the baryon mass with the chiral symmetry restoration in dense QCD is proposed in the framework of AdS/QCD model as the phenomenological bottom-up constructions, called the “hard-wall” model [37].

Next we analyze the RMS mass radius of the baryon for the Skyrme model and the BIS model. By using the normalized energy density  $\bar{\varepsilon}(r) \equiv \varepsilon(r)/E$  ( $\varepsilon(r)$  is the total energy density and  $E$  is the mass of single baryon), the

RMS mass radius can be naturally introduced on  $S^3$  with radius  $R$  as

$$\begin{aligned} \sqrt{\langle r^2 \rangle} &= \left[ \int_{S^3} d^3x \cdot \bar{\varepsilon}(r) r^2 \right]^{1/2} \\ &\equiv \left[ \int_0^{\pi R} 4\pi dr R^2 \sin^2 \frac{r}{R} \cdot \bar{\varepsilon}(r) r^2 \right]^{1/2}, \end{aligned} \quad (70)$$

where  $R^2 \sin^2 \frac{r}{R}$  denotes the measure of the curved manifold  $S^3$ . In the case of the identity map, the RMS mass radius can be analytically calculated by using the normalized uniform energy density for the identity map:  $\bar{\varepsilon}_{\text{id}} \equiv 1/2\pi^2 R^3$  as

$$\begin{aligned} \sqrt{\langle r^2 \rangle}_{\text{id}} &\equiv \left[ \int_0^{\pi R} 4\pi dr R^2 \sin^2 \frac{r}{R} \cdot \bar{\varepsilon}_{\text{id}} r^2 \right]^{1/2} \\ &= \pi R \sqrt{\frac{1}{3} - \frac{1}{2\pi^2}}. \end{aligned} \quad (71)$$

In Fig. 8, we show the RMS mass radius for the Skyrme model and the BIS model with radius  $R$  of  $S^3$ . One can find that the RMS mass radius in each model increases nonlinearly around its critical radius as  $R$  decreases, indicating the swelling phenomenon of the baryon in the high density phase. Such swelling of the baryon can also be seen in the analysis of the Skyrme crystal on the three-dimensional cubic lattice [26] and also the finite density bag model [59]. After the delocalization phase transition, the energy density of a single baryon is uniformly saturated over the surface of  $S^3$ . Then the RMS mass radius decreases linearly with the decrease of  $R$  as seen in Eq. (71). (In the uniform phase, baryons are no longer localized, and the RMS mass radius may have less physical meaning.)

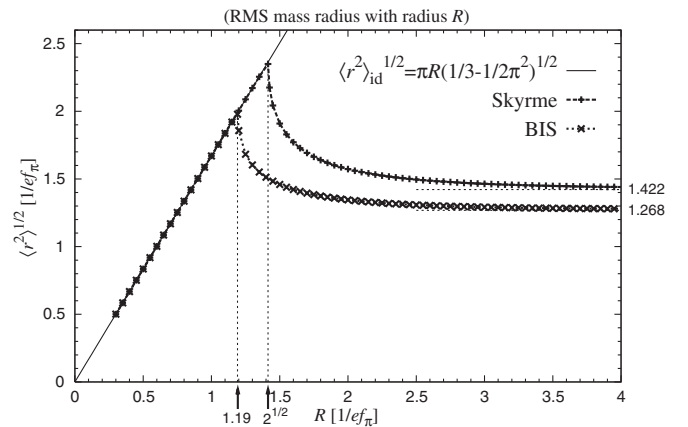


FIG. 8. RMS mass radius of a single baryon for the identity map, the Skyrme model, and the BIS model with radius  $R$  of  $S^3$ . The variables “1.422” and “1.268” are the RMS mass radius of the baryon on the flat space  $\mathbf{R}^3$  for the Skyrme model and the BIS model, respectively.

#### D. Swelling mechanism and its phenomenological implications

In the previous section, we numerically find the swelling of the baryon by taking the Skyrme picture for the baryon analysis. Actually, as discussed in Sec. III A, the Skyrme picture is naturally derived from QCD through the new concept of holography. Therefore, one can expect the swelling phenomenon in QCD itself. In this section, we try to give a qualitative explanation about the swelling mechanism of a baryon in terms of QCD, by especially referring to contexts of the lattice QCD [42] and also the finite density bag picture [59].

First, in lattice QCD study, the nonperturbative QCD vacuum is analyzed within a finite box of periodic boundaries (and also Dirichlet boundaries) in the Euclidean space. The nonperturbative effects with long wavelength tend to be “blocked out” from such finite box of definite boundaries, so that the QCD vacuum in the finite box is found to approach the perturbative one. Also, the finite-temperature phase transition in lattice QCD occurs because of the definite boundaries along the imaginary time axis in Euclidean space; as the temperature increases, the QCD vacuum in the Euclidean space is more closely packed along the imaginary time axis to block out the nonperturbative effects with long wavelength, which eventually gives the transition into the perturbative QCD vacuum, like the chiral symmetry restoration and also the deconfinement.

Next we combine the above picture into the finite density bag model, to explain the mechanism of the swelling in QCD. In the bag model, the baryon is represented by a “bag” with the perturbative QCD vacuum surrounded by the Dirichlet boundaries, which is supported by the nonperturbative QCD vacuum with the bag pressure as shown in Fig. 9(a). As a number of bags increases, representing the high density baryonic matter, the nonperturbative QCD

vacuum around the bags is more closely packed within a definite region, imitated by a cube with dashed lines in Fig. 9(b). Then, in analogy with the case of lattice QCD study discussed above, the QCD vacuum around the bags should approach the perturbative one by blocking out the nonperturbative effects with long wavelength as shown by the several waves in Fig. 9. Therefore, the bag pressure as a nonperturbative effect decreases as the number of bags increases, so that it eventually gives the swelling of bags. Such swelling in turn decreases the region of nonperturbative QCD vacuum around the bags to give the decrease of the bag pressure again. In this sense, such swelling could occur *nonlinearly* as shown in Fig. 8, giving some drastic change of features like deconfinement in the baryonic matter. One can expect some resemblance between the finite density bag model and the Skyrme matter in our study with respect to baryonic matter, so that the swelling phenomenon as shown in Fig. 8 could be understood on the same footing provided above.

Now we also suggest the physical effects of the swelling in the high-density baryonic matter. Here we take into account possible baryon excitation with the chiral soliton picture. Since a moment of inertia of the baryon is related with the size of the baryon, some nonlinear increase in the moment of inertia around critical density is expected along with the swelling of a baryon. In the semiclassical quantization procedure of a Skyrme soliton, the baryon mass spectra is given [43] as

$$M_J = M_{\text{HH}} + \frac{J(J+1)}{2I}, \quad (72)$$

where  $M_{\text{HH}}$  is the static hedgehog mass and  $I$  is the moment of inertia of a baryon. The quantum number  $J$  in Eq. (72) denotes the spin  $S$  and the isospin  $I$  of the baryon as  $J(=S=I) = \frac{1}{2}$  for  $N$  and  $J(=S=I) = \frac{3}{2}$  for  $\Delta$ . The baryon mass splitting in the second term in Eq. (72) is

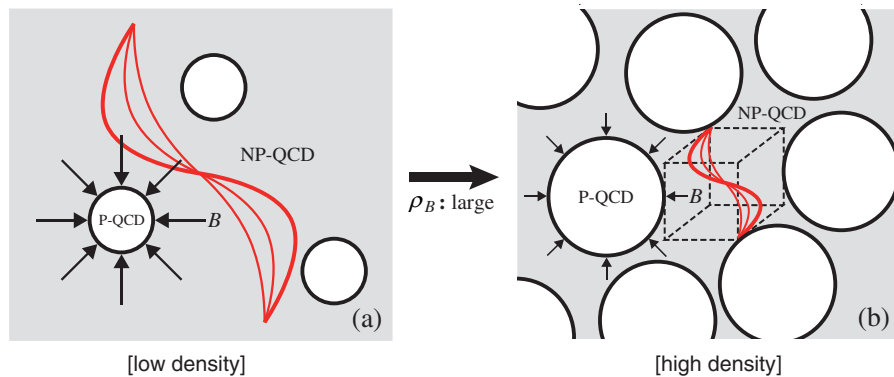


FIG. 9 (color online). Schematic figure of the finite density bag model for low density case (a) and high density case (b): the baryon is represented by a bag with perturbative QCD vacuum (P-QCD) surrounded by Dirichlet boundaries, supported by the nonperturbative QCD vacuum (NP-QCD) with the bag pressure  $B$ . Several waves in (a) and (b) represent the nonperturbative effects of QCD with a certain wavelength. A cube with dashed lines in (b) imitates a definite region of nonperturbative QCD vacuum surrounded by the surfaces of the bags with Dirichlet boundaries, to discuss the mechanism of swelling in the high density baryonic matter.

proportional to the inverse of the moment of inertia, indicating that a larger object cannot be easily rotated. Therefore we can now propose that the baryon mass splitting decreases as the density increases in the medium, because the moment of inertia  $I$  increases due to the swelling. In other words, the *individuality* of each baryon like  $N$ ,  $\Delta$ , etc., would be *lost* at least with respect to their mass spectra as the density increases. Such loss of individuality may be regarded as some precursory phenomena of deconfinement, where the dominant degrees of freedom in the hadronic matter shifts from the confined composites as baryons (and mesons) into quarks and gluons.

Such swelling of the baryon leads to some interesting phenomenological realizations. As one possibility, here we propose the stable  $N$ - $\Delta$  mixed matter in dense QCD. For simplicity, we consider the ‘‘symmetric nuclear matter,’’ where only the strong interaction is taken into account without the electromagnetic interaction. In the low density case, there exists large  $N$ - $\Delta$  splitting as  $(M_\Delta - M_N) \sim 290$  MeV, and the Fermi surface of the nucleons  $\mu_N$  may locate below the threshold of  $\Delta$  isobars, i.e., its mass  $M_\Delta$ . This situation gives only the nucleon degrees of freedom as nuclear matter. Now, if the swelling occurs as the density increases, the  $N$ - $\Delta$  splitting should decrease as discussed in Eq. (72). Then, the Fermi surface of the nucleons  $\mu_N$  would exceed  $M_\Delta$  to give the  $\Delta$  isobar degrees of freedom in the medium through the equilibrium process  $N + \pi \leftrightarrow \Delta$ . In this sense,  $N$ - $\Delta$  mixed matter would be realized in dense QCD because of the swelling of a baryon. Such  $N$ - $\Delta$  mixed matter may appear in the deep interior of neutron stars between the nuclear crust and the core of quark matter as the precursor of deconfinement, giving some softening of the EOS of neutron stars relative to the analysis without the mixed matter. While these are qualitative discussions, we feel that these explanations catch some essential aspects of baryonic matter with baryon excitation in view of its swelling nature.

## V. PHASE TRANSITIONS WITH ORDER PARAMETERS

In this section we discuss the delocalization phase transition in view of the deconfinement, and also the chiral symmetry restoration by introducing the proper order parameters in the Skyrme model and the BIS model. The relations between these phase transitions are also considered by referring to other QCD phenomenologies in the end of Sec. VB.

### A. Delocalization phase transition

First we consider the delocalization phase transition with the order parameter. By using the normalized energy density  $\bar{\varepsilon}(\mathbf{x}) \equiv \varepsilon(\mathbf{x})/E$  ( $\varepsilon(\mathbf{x})$  is total energy density and  $E$  is the mass of single Skyrmion), one can introduce the spatial fluctuation  $\Phi(R)$  of the energy density around the uniform energy density distribution [60] as

$$\Phi(R) \equiv \frac{1}{2} \int_{S^3} d^3x |\bar{\varepsilon}(\mathbf{x}) - \bar{\varepsilon}_{\text{id}}|, \quad (73)$$

where  $\bar{\varepsilon}_{\text{id}} \equiv \frac{1}{2\pi^2 R^3}$  is the normalized uniform energy density for the identity map. If the Skyrmion is well localized like the delta function, the energy density  $\bar{\varepsilon}(\mathbf{x})$  is almost decoupled with uniform energy density distribution  $\bar{\varepsilon}_{\text{id}}$  through the spatial integral over  $S^3$ . Therefore, its spatial fluctuation  $\Phi(R)$  becomes

$$\Phi(R) \sim \frac{1}{2} \int_{S^3} d^3x \{|\bar{\varepsilon}(\mathbf{x})| + |\bar{\varepsilon}_{\text{id}}|\} = 1. \quad (74)$$

On the other hand, if the Skyrmion gives uniform energy density distribution as the identity map, the energy density  $\bar{\varepsilon}(\mathbf{x})$  coincides with  $\bar{\varepsilon}_{\text{id}}$ , giving

$$\Phi(R) = 0. \quad (75)$$

In this sense,  $\Phi(R)$  in Eq. (73) measures the amount of localization in the energy density distribution of the Skyrmion, regarded as the order parameter of delocalization phase transition in the baryonic matter.

In Fig. 10, we show the value of  $\Phi(R)$  for the Skyrme model and the BIS model with radius  $R$  of  $S^3$ . For sufficiently large  $R$  as the low density state, the Skyrme soliton is well localized for both the Skyrme model and the BIS model, giving  $\Phi(R) \sim 1$ . With the decrease of  $R$ , the baryon tends to delocalize with the decrease of  $\Phi(R)$ , regarded as some medium effects in the baryonic matter. The delocalization phase transition into the uniform phase with  $\Phi(R) = 0$  occurs at the critical radius  $R = R_{\text{crit}}^{\text{Skyrme}} = \sqrt{2}$  for the Skyrme model and at  $R = R_{\text{crit}}^{\text{BIS}} = 1.19$  for the BIS model. Actually, the delocalization phase transition in the BIS model is delayed along with the decrease of  $R$  because of the heavy  $\rho$  mesons in the core region of the baryon, discussed in Sec. IVA.

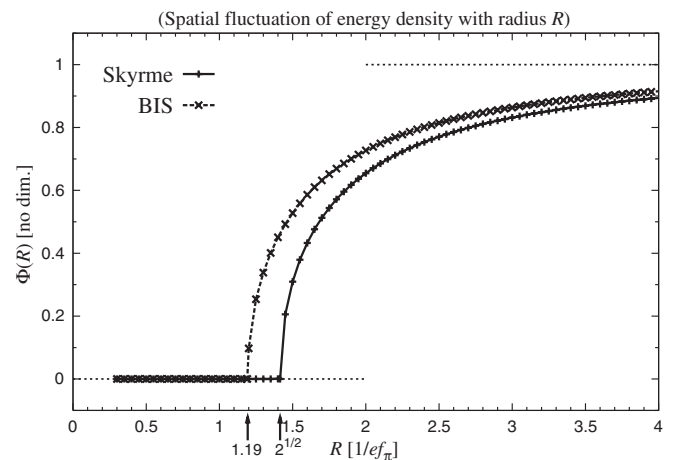


FIG. 10. Spatial fluctuation  $\Phi(R)$  of the energy density of a single baryon for the Skyrme model and the BIS model with radius  $R$  of  $S^3$ .

Here one may have some temptation to relate the delocalization phase transition with the deconfinement of the baryon in QCD, which should be carefully discussed. Actually, there have been several conflicts about the meaning of the delocalization phase transition in the standard Skyrme model with finite density [26,27,60–62]. Within the traditional works in the 1970's, the direct linking of the Skyrme model with QCD was still uncertain. Furthermore, the standard Skyrme model does not manifestly include quarks and gluons, so that great care should be taken to relate the delocalization of the Skyrmion with the deconfinement of the baryon as the appearance of quark-gluon dynamics. In our case, however, the new concept of holography allows us to derive the Skyrmion picture from QCD itself, which is discussed in Sec. III A. Moreover, one should also note that quark degrees of freedom can be represented by pions, suggested in some QCD phenomenologies with “Cheshire cat picture” as in the chiral quark model [54,55] derived from the bosonization scheme for QCD. With these backgrounds, here we propose that the delocalization phase transition in the BIS model can be more admissibly related with the deconfinement of the baryons in QCD, relative to the standard Skyrme models in the 1970's.

## B. Chiral symmetry restoration in nonlinear realization

Next we consider the chiral symmetry restoration with the order parameter. Normally, in the case of the linear sigma model, the chiral symmetry restoration can be signaled by the vanishing of the expectation value of the meson fields at the matter ground state as

$$\langle \sigma(x_\mu)^2 + \mathbf{\Pi}(x_\mu)^2 \rangle^* = 0, \quad (76)$$

where the sigma meson field  $\sigma(x_\mu)$  and three pseudoscalar pion fields  $\mathbf{\Pi}(x_\mu)$  are called the “linear” realization of chiral symmetry. We relate this terminology to the nonlinear sigma model, since the meson effective action and also the Skyrmion picture are based on the “nonlinear” realization of the chiral symmetry. In the nonlinear sigma model, the meson fields  $\sigma(x_\mu)$  and  $\mathbf{\Pi}(x_\mu)$  are introduced from the chiral field  $U(x_\mu) \in \text{SU}(N_f)_A$  as

$$\begin{aligned} U(x_\mu) &= e^{i\tau_a \pi_a(x_\mu)/f_\pi} \cos\{|\pi|/f_\pi\} + i\tau_a \hat{\pi}_a \sin\{|\pi|/f_\pi\} \\ &\equiv \{\sigma(x_\mu) + i\boldsymbol{\tau} \cdot \mathbf{\Pi}(x_\mu)\}/f_\pi \\ (|\pi| &\equiv \sqrt{\pi_a \pi_a}, \hat{\pi}_a \equiv \pi_a/|\pi|) \end{aligned} \quad (77)$$

Since  $U(x_\mu)$  is a unitary matrix with the condition  $U^\dagger(x_\mu)U(x_\mu) = 1$ , the squared sum of the meson fields  $\sigma(x_\mu)$  and  $\mathbf{\Pi}(x_\mu)$  in Eq. (77) should be constant everywhere as

$$\sigma(x_\mu)^2 + \mathbf{\Pi}(x_\mu)^2 = f_\pi^2. \quad (78)$$

Therefore, as far as the action is written in the chiral field  $U(x_\mu)$  with fixed  $f_\pi$ , the meson fields  $\sigma(x_\mu)$  and  $\mathbf{\Pi}(x_\mu)$  are

forced on a surface of a three-dimensional closed manifold  $S^3_{\text{int}}$  with finite radius  $f_\pi$  in the internal space. In fact, the existence of such closed manifold  $S^3_{\text{int}}$  is essential for the concept of a Skyrmion, which is a nontrivial winding of the compactified physical manifold  $S^3$  around the other closed manifold  $S^3_{\text{int}}$  with conserved topological charge, belonging to the homotopical classification  $\pi_3(S^3) = \mathbf{Z}$  [63]. However, by comparing Eq. (78) with Eq. (76), one would always encounter a problem of how to describe the chiral symmetry restoration with its nonlinear realization.

Now in this paper, we take a spatially-averaged condensate of the meson fields  $\sigma(x_\mu)$  and  $\mathbf{\Pi}(x_\mu)$  as the order parameter of the chiral symmetry restoration with the nonlinear realization [62] as

$$\{\langle \sigma(x_\mu) \rangle^2 + \langle \mathbf{\Pi}(x_\mu) \rangle^2\}/f_\pi^2. \quad (79)$$

Here, the bracket in Eq. (79) denotes the three-dimensional spatial average in the medium with volume  $V$  as

$$\langle \Theta(x_\mu) \rangle \equiv \frac{\int_V d^3x \Theta(x_\mu)}{\int_V d^3x}. \quad (80)$$

Such spatially-averaged condensate of the meson fields is somehow similar to the spatially-averaged magnetization  $\langle \mathbf{M}(\mathbf{x}) \rangle$  as the global order parameter of the ferromagnetic material like bulk iron. Within the bulk iron at sufficiently high temperature, the spins of the ions orient randomly to get the entropy gain in the free energy. As the temperature decreases below the critical temperature without the external magnetic field, there appear magnetic domains with nonzero local magnetization  $\mathbf{M}(\mathbf{x}) \neq 0$ . However, because of the total angular momentum conservation, the spatially-averaged magnetization  $\langle \mathbf{M}(\mathbf{x}) \rangle$  should vanish with the appearance of a complex structure of magnetic domain walls within the bulk iron, which gives *no* breaking of the global spatial symmetry macroscopically in the bulk material as  $\langle \mathbf{M}(\mathbf{x}) \rangle = 0$ . In this sense, the spatially-averaged condensate of the meson fields in Eq. (79) can be regarded as the “global” order parameter of the chiral symmetry in the bulk hadronic matter.

By taking the hedgehog configuration Ansatz  $\pi_a(x_\mu)/f_\pi = \hat{x}_a F(r)$  as in Eq. (35), the meson fields  $\sigma(x_\mu)$  and  $\mathbf{\Pi}(x_\mu)$  can be written as

$$\sigma(x_\mu)/f_\pi = \cos\{\pi(x_\mu)/f_\pi\} = \cos F(r), \quad (81)$$

$$\mathbf{\Pi}(x_\mu)/f_\pi = \hat{\pi} \sin\{\pi(x_\mu)/f_\pi\} = \hat{x} \sin F(r). \quad (82)$$

Note here that the pion field with the hedgehog ansatz in Eq. (82) is proportional to the unit directional vector  $\hat{x}$ , so that its spatial average becomes trivially zero. Therefore, only the sigma meson field should be considered as the global order parameter of the chiral symmetry. If a Skyrmion is well localized around the north pole at  $r = 0$  on the manifold  $S^3$ , the classical meson field configuration  $F(r)$  becomes zero almost everywhere except for the

localized point  $r \sim 0$ . Therefore the sigma meson configuration in Eq. (81) becomes  $\sigma(x_\mu)/f_\pi \sim 1$  almost everywhere. In other words, the vacuum is so much oriented even globally in the medium, thus its spatial average becomes nonzero as

$$\langle \sigma(x_\mu) \rangle / f_\pi \sim 1, \quad (83)$$

indicating the appearance of the chiral symmetry broken phase. On the other hand, if the Skyrme gives uniform energy density distribution as the identity map  $F(r) = \pi - r/R$  in Eq. (67), the sigma meson configuration becomes  $\sigma(x_\mu)/f_\pi = \cos \frac{r}{R}$ , changing monotonously from  $-1$  to  $1$  over the coordinate space  $S^3$  through the arc distance  $r \in [0, \pi R]$ . Therefore, its spatial average vanishes as

$$\langle \sigma(x_\mu) \rangle / f_\pi = 0, \quad (84)$$

indicating the appearance of the chiral symmetry restored phase. These considerations about Eqs. (83) and (84) also indicate that the chiral symmetry restoration is indirectly related with the energy density distribution in the hadronic matter through the classical meson field configurations.

In Fig. 11, we show the spatially-averaged condensate  $\langle \sigma(x_\mu) \rangle / f_\pi$  for the Skyrme model and the BIS model with radius  $R$  of  $S^3$ . The spatial average with the hedgehog configuration (81) is explicitly taken for each closed manifold  $S^3$  as

$$\begin{aligned} \langle \sigma(x_\mu) \rangle / f_\pi &= \langle \cos F(r) \rangle = \frac{\int_{S^3} d^3x \cos F(r)}{\int_{S^3} d^3x} \\ &= \frac{\int_0^{\pi R} 4\pi dr R^2 \sin^2 \frac{r}{R} \cdot \cos F(r)}{2\pi^2 R^3}. \end{aligned} \quad (85)$$

For sufficiently large  $R$  as the low density state, the Skyrme soliton is well localized for both the Skyrme model and the BIS model, as previously shown in Fig. 10. Therefore, as discussed in Eq. (83), the spatially-averaged condensate of

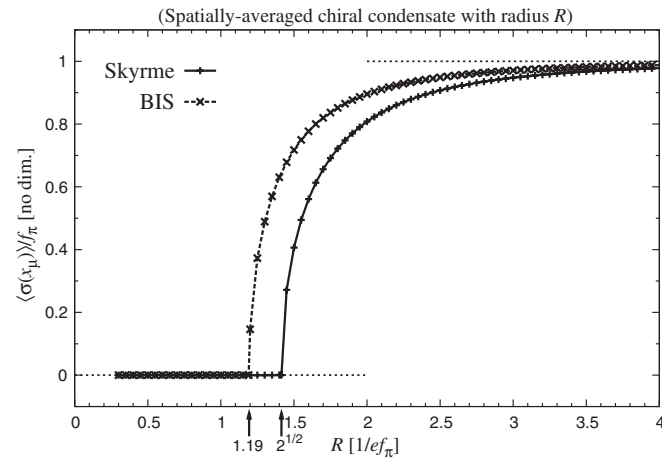


FIG. 11. Spatially-averaged condensate of the sigma meson field  $\langle \sigma(x_\mu) \rangle / f_\pi$  of a single baryon for the Skyrme model and the BIS model with radius  $R$  of  $S^3$ .

the meson field becomes  $\langle \sigma(x_\mu) \rangle / f_\pi \sim 1$  as the chiral symmetry breaking in both models as shown in Fig. 11. In this sense, the  $\rho$  meson field (and also the other vector and axial vector meson fields, if they are included) would have less importance for the chiral symmetry breaking in the bulk hadronic matter as far as sufficiently localized baryon appears in the medium. With the decrease of  $R$ ,  $\langle \sigma(x_\mu) \rangle / f_\pi$  monotonously decreases, which corresponds to the partial chiral symmetry restoration as the medium effect in the baryonic matter. The chiral symmetry is fully restored with  $\langle \sigma(x_\mu) \rangle / f_\pi = 0$  at the critical radius  $R = R_{\text{crit}}^{\text{Skyrme}} = \sqrt{2}$  for the Skyrme model and at  $R = R_{\text{crit}}^{\text{BIS}} = 1.19$  for the BIS model. Actually, the small radius  $R$ , i.e., the larger baryon-number density, is needed to give the chiral symmetry restoration due to the  $\rho$  meson fields, similar to the case of the delocalization phase transition as previously discussed.

Finally, we comment on the relation between the deconfinement and the chiral symmetry restoration in QCD, which has been discussed so long in the hadron physics. The relation between two phase transitions is nontrivial since they are characterized by the different symmetries: the global chiral symmetry  $SU(N_f)_L \times SU(N_f)_R$ , and  $Z(3)$  symmetry as the center of the  $SU(3)_c$  gauge group. Note that the former can be defined in the massless quark limit, while the latter in the heavy quark limit, leading to difficulties in discussing their relation.

Despite the difficulties, several implications have been obtained: In finite temperature, the lattice QCD studies suggest that the two phase transitions occur at the same critical temperature  $T_c \sim 170$  MeV [42]. Such simultaneous occurrence is supported by the analyses of the Nambu-Jona-Lasinio model with a Polyakov loop (PNJL model) as a low-energy effective theory of QCD [64]. Actually, these two phase transitions are separated with respect to their dominant symmetries as mentioned above, so that such mysterious coherence between two phase transitions is often compared to some kinds of “entanglement” [64]. Furthermore, the simultaneous occurrence of the two phase transitions is also suggested by the recent analysis of the holographic QCD with D4/D8/ $\overline{D8}$  multi-D brane configurations: two independent chirality spaces on the D8 and  $\overline{D8}$  branes, respectively, are connected with each other (chiral symmetry breaking) by the “worm hole” of the D4 supergravity background into which the colored objects like quarks and gluons are absorbed (color confinement) [9]. In this sense, these two phase transitions are more directly related with each other as just a single event on the “worm hole” in the extra dimensions, the effects of which might appear as some kind of mysterious entanglement in view of the four-dimensional space-time.

Now, the situation has not been clear in finite density. In this work, we indirectly relate the two phase transitions through the meson field configurations. Admittedly, our approach includes only meson fields and baryons appear as

mesonic solitons. However, if the Cheshire cat picture holds and quark-gluon dynamics can be indirectly expressed in the meson dynamics as an effective model, our results could be interpreted as the simultaneous occurrence of two phase transitions in the finite density QCD. Investigations in this direction are interesting and should be developed further.

## VI. CRITICAL DENSITY WITH PHYSICAL UNITS

In this section, we show the critical densities of the phase transitions for the Skyrme model and the BIS model with recovering the physical units.

In this study, a single baryon is placed on a closed manifold  $S^3$  with the surface volume  $2\pi^2 R^3$ , so that the total baryon-number density  $\rho_B$  can be given as

$$\rho_B = (2\pi^2 R^3)^{-1} (ef_\pi)^3 [\text{fm}^{-3}]. \quad (86)$$

Now, in the holographic model, by fixing two parameters, e.g., experimental inputs for  $f_\pi$  and  $m_\rho$ , all the physical quantities like masses and the coupling constants are uniquely determined, which is a remarkable consequence of the holographic approach discussed in Sec. II. First, we take  $f_\pi$  and  $m_\rho$  as experimental values,

$$f_\pi = 92.4 \text{ MeV}, \quad m_\rho = 776.0 \text{ MeV}. \quad (87)$$

Then the Skyrme parameter  $e$  in Eq. (42) can be uniquely determined as

$$e \simeq 7.315. \quad (88)$$

With these experimental inputs, we show in Fig. 12 the total baryon-number density  $\rho_B$  in Eq. (86) as a function of

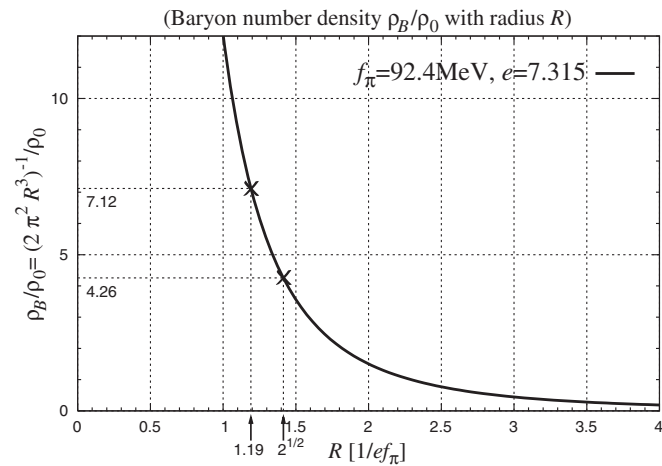


FIG. 12. Total baryon-number density  $\rho_B$  in Eq. (86) with radius  $R$  of  $S^3$ , where the experimental inputs are taken as  $f_\pi = 92.4$  MeV and  $e = 7.315$  in Eqs. (87) and (88). The vertical axis is given as  $\rho_B$  divided by the normal nuclear density  $\rho_0 \simeq 0.17 \text{ fm}^{-3}$ . Critical densities of the phase transitions for the Skyrme model and the BIS model are also shown for each critical radius as  $R_{\text{crit}}^{\text{Skyrme}} = \sqrt{2}$  and  $R_{\text{crit}}^{\text{BIS}} = 1.19$ .

radius  $R$  of  $S^3$ , divided by the normal nuclear density  $\rho_0 \simeq 0.17 \text{ fm}^{-3}$ . From Fig. 12 and also Eq. (86), the critical densities for the Skyrme model ( $R_{\text{crit}}^{\text{Skyrme}} = \sqrt{2}$ ) and the BIS model ( $R_{\text{crit}}^{\text{BIS}} = 1.19$ ) are found as follows:

$$\rho_B^{\text{Skyrme}} \equiv \{2\pi^2 (R_{\text{crit}}^{\text{Skyrme}})^3\}^{-1} (ef_\pi)^3 \simeq 4.26\rho_0, \quad (89)$$

$$\rho_B^{\text{BIS}} \equiv \{2\pi^2 (R_{\text{crit}}^{\text{BIS}})^3\}^{-1} (ef_\pi)^3 \simeq 7.12\rho_0. \quad (90)$$

The heavy  $\rho$  meson fields in the core region of the baryon tend to decrease the total size of the baryon [9], so that the  $\rho$  meson field has a significant role to increase the critical density into the uniform phase as in Eq. (90) relative to Eq. (89).

In Sec. IV A, we discuss the disappearance of the  $\rho$  meson field in the high density phase of baryonic matter, while we now find the significant roles of the  $\rho$  meson field as for the critical density in Eq. (90) relative to Eq. (89). This situation somehow resembles the “two-Higgs model” with scalar fields  $\phi$  and  $\chi$  in the finite temperature. On the critical temperature of a phase transition with the dynamics of a scalar field  $\chi$ , the condensate of the  $\chi$  field might become trivial as  $\langle\chi\rangle = 0$ . However, in general, the mass of the  $\chi$  field and also the interactions between the  $\chi$  and  $\phi$  fields affect the critical properties like critical temperature. In this sense, even if the  $\rho$  meson fields disappear near the critical point, they could affect the critical phenomena as in Eq. (90) through its mass and also the interactions with pions in the action  $S_{\text{eff}}$  in Eq. (19).

Here we briefly comment on the value of the critical density by taking the other parameter set used by Adkins *et al.* [25]. In 1983, Adkins *et al.* analyzed the baryon mass spectra with the semiclassical quantization of the Skyrme model, whereas the  $N$ - $\Delta$  splitting corresponds to the higher order contribution  $O(N_c^{-1})$  relative to the static Skyrme action  $O(N_c^1)$  in the large- $N_c$  expansion. To reproduce the proper amount of the  $N$ - $\Delta$  splitting, they take the smaller pion decay constant and Skyrme parameter [25] as

$$f_\pi = 64.5 \text{ MeV}, \quad e = 5.44. \quad (91)$$

Now if the parameter set in Eq. (91) is used for the baryon-number density in Eq. (86), we find too small critical density ( $\sim 0.6\rho_0$ ) for the Skyrme model. If one can relate the phase transition in the Skyrme model with the deconfinement of the baryon in QCD, it might propose, e.g., that quark degrees of freedom are already manifest in the normal nuclei. This unreasonable results may come from the fact that semiclassical quantization procedure corresponds to extracting higher order contributions  $O(N_c^{-1})$  from the leading order Skyrme action  $O(N_c^1)$  as for the large- $N_c$  expansion.

The same comments can also be applied to the holographic model if one tries to perform the semiclassical quantization as the baryon analysis. In fact, holographic QCD is derived as the large- $N_c$  effective theory even by starting from superstring framework. Higher order effects

of the large- $N_c$  expansion like the baryon mass splitting correspond to the string loop effects beyond the classical supergravity, which should be fairly intractable. With these considerations above, we do not intentionally proceed to the semiclassical quantization of Skyrme soliton in the present work, and we employ the experimental inputs (87) and Skyrme parameter (88) in the analysis of the critical densities with recovering the physical units. Actually, due to the scaling property of the BIS model discussed in Sec. II, all the results in ANW units in the previous sections should not be altered, being independent of the definite values for  $f_\pi$  and  $m_\rho$ .

## VII. SUMMARY AND OUTLOOK

We have studied baryonic matter in holographic QCD with D4/D8/ $\overline{D8}$  multi-D brane configurations, by analyzing the system of a single brane-induced Skyrminion on the three-dimensional closed manifold  $S^3$ . By changing the size of  $S^3$ , the density dependence of the baryon properties are examined from a holographic point of view.

First we begin with the Dirac-Born-Infeld (DBI) action of the probe D8 brane with D4 supergravity background. With the dimensional reductions, we get the five-dimensional Yang-Mills action with a curved fifth dimension, as the leading order of the large- $N_c$  and large 'tHooft coupling expansions in dual nonperturbative (strong-coupling) QCD. Through the mode expansions of the five-dimensional gauge fields, we get the four-dimensional meson effective action from holographic QCD. In particular, we emphasize the appearance of the ultraviolet cutoff scale  $M_{\text{KK}} \sim 1$  GeV in the holographic approach to be dual of QCD. Therefore, we construct the four-dimensional meson effective action with pion and  $\rho$  meson fields below the cutoff scale  $M_{\text{KK}}$ .

Next we discuss the baryon in holographic QCD as the ‘‘brane-induced Skyrminion’’ in the four-dimensional meson effective action. The analyses of the baryon in the meson effective action with restricted degrees of freedom below the cutoff scale  $M_{\text{KK}}$  is called the ‘‘truncated-resonance model’’ for the baryon. Taking the hedgehog configuration Ansatz for pion and  $\rho$  meson fields, we can investigate many properties of a single baryon as the brane-induced Skyrminion, which are inclusively summarized in Ref. [9].

Then we consider the baryonic matter in holographic QCD, as the extension of the holographic approach to dense QCD. Specifically, we treat the baryonic matter with large- $N_c$ , because holographic QCD is derived as the large- $N_c$  effective theory, in dual of the classical supergravity. For sufficiently large  $N_c$ , the kinetic energy and the quantum effects can be suppressed relative to the static mass from simple large- $N_c$  countings [8], where the baryonic matter comes into the static Skyrme matter. In this sense, we analyze the static Skyrme matter to see the typical features of the baryonic matter with large- $N_c$  conditions.

In order to analyze the static Skyrme matter on the flat coordinate space  $\mathbf{R}^3$ , we alternately treat the system of a single brane-induced Skyrminion on the three-dimensional closed manifold  $S^3$ . The interactions between the baryons are simulated by the curvature of the closed manifold  $S^3$ , and, as the size of  $S^3$  decreases, the baryon-number density increases in this modeling. Actually, through the projection procedure from the flat space  $\mathbf{R}^3$  onto the curved space  $S^3$ , we get the hedgehog mass and also the Euler-Lagrange equations for pion and  $\rho$  meson fields of the brane-induced Skyrminion on  $S^3$ .

By numerically solving the Euler-Lagrange equations for pion and  $\rho$  meson fields on  $S^3$ , we find a stable soliton solution as the brane-induced Skyrminion on  $S^3$ . By using this solution, we analyze many properties of the baryon within the baryonic matter. Especially by comparing the standard Skyrme model without  $\rho$  mesons and the brane-induced Skyrme (BIS) model, the roles of (axial) vector mesons in dense QCD are discussed from a holographic point of view.

First we show the baryon-number density dependence of the energy density and the field configuration profiles of a single baryon by changing the size of  $S^3$ . As the size of  $S^3$  decreases, the localized energy density distribution of a single baryon becomes uniform as the identity map, which is called the ‘‘delocalization phase transition.’’ The critical radii of the phase transitions are given as  $R = R_{\text{crit}}^{\text{Skyrme}} = \sqrt{2}[\frac{1}{ef_\pi}]$  for the Skyrme model and  $R = R_{\text{crit}}^{\text{BIS}} = 1.19[\frac{1}{ef_\pi}]$  for the BIS model. Because of the shrinkage of the baryon size due to the  $\rho$  meson effects [9], the smaller critical radius of  $S^3$ , i.e., the larger baryon-number density is needed for the BIS model to give the delocalization phase transition. We also find that the  $\rho$  meson field absolutely disappears and only the pion field survives near the critical density. Then, with the mathematical arguments, we propose a remarkable conjecture that all the (axial) vector meson fields would disappear and only the pion field survives near the critical density, referred as the ‘‘pion dominance’’ in dense baryonic matter.

We also investigated the baryon-number density dependence of the mass and the root-mean-square (RMS) mass radius of single baryon. We find the swelling phenomenon of the baryon, as the nonlinear increase of the RMS mass radius near the critical density. Actually, the nonperturbative QCD vacuums around the baryons are closely packed as the baryon-number density increases. Therefore, the nonperturbative effect with long wavelength like the bag pressure is blocked out from such definite region to give the swelling of the baryon. Such swelling provides the decrease of the baryon mass splitting, indicating the loss of the individualities for the baryons as the precursor of the deconfinement. We also propose the stable  $N$ - $\Delta$  mixed matter in dense QCD because of the swelling, which could, e.g., soften the EOS of the neutron stars.

The features of the delocalization phase transition and the chiral symmetry restoration are also analyzed with the order parameters in the holographic QCD. We conjecture with careful arguments that the delocalization phase transition can be related with the deconfinement of the baryons in QCD. Then we find the coherence of the deconfinement and the chiral symmetry restoration through the meson field configurations. Such coherence of the two phase transitions are also suggested in the lattice QCD study in the finite temperature [42], the PNJL model as a low-energy effective theory of QCD [64], and also the Sakai-Sugimoto model as one of the reliable holographic approaches [9].

We also calculate the critical densities of the phase transitions with the experimental inputs for the pion decay constant  $f_\pi$  and  $\rho$  meson mass  $m_\rho$  as  $f_\pi = 92.4$  MeV and  $m_\rho = 776.0$  MeV. We find the critical densities as  $\rho_B^{\text{Skyrme}} \simeq 4.26\rho_0$  for the Skyrme model and  $\rho_B^{\text{BIS}} \simeq 7.12\rho_0$  for the BIS model. We can see that the larger baryon-number density is needed for the BIS model to give the phase transitions because of the shrinkage of total size of the baryon with heavy  $\rho$  mesons in its core region.

Finally, we compare our truncated-resonance approach for the baryons with the other works of baryons as the *instantons* in holographic QCD. In fact, there seem to exist some conflicts for the baryon analysis in holographic QCD, especially between the truncated-resonance model and the instanton models. In Refs. [11–14], the baryons are studied as the instantons on the five-dimensional gauge theory of the probe D8 brane with D4 supergravity background as the holographic dual of QCD. The properties of the baryonic matter are also analyzed by the system of the single instanton on the three-dimensional closed manifold  $S^3$  as the Wigner-Seitz approximation [15]. In these analyses, the instanton is found to shrink into zero size only for the DBI sector of the effective action of the D8 brane, which corresponds to the leading order of large- $N_c$  and large 'tHooft coupling expansions. In the holographic approach, an infinite tower of color-singlet modes with mesonic quantum numbers as  $\rho, a_1, \rho', a_1', \rho'', \dots$ , appears in the mode expansions of the five-dimensional gauge field  $A_\mu(x, z)$  on the D8 brane as in Eq. (7). In this sense, the baryon as the instanton on the five-dimensional gauge theory before the mode expansion is, in principle, to be composed by the infinite tower of such color-singlet modes with mesonic quantum numbers. Therefore, the instability of the instanton only with the DBI sector is often regarded that the infinite number of (axial) vector mesons  $\rho, a_1, \rho', a_1', \rho'', \dots$ , would affect the low-energy soliton feature to give the zero size. Then, in order to describe the baryon as an instanton with finite size in the holographic approach, the inclusion of the Chern-Simons (CS) sector of the effective action of the D8 brane is claimed, whereas the CS sector corresponds to the higher order contribution of the 'tHooft coupling expansion relative to the DBI sector.

However, as emphatically noted in Sec. II, the appearance of certain cutoff scales like  $M_{\text{KK}} \sim 1$  GeV should be essential for the holographic model to be dual of QCD. In fact, the mesonic mass spectra predicted from holographic QCD starts to deviate from the experimental data beyond the  $M_{\text{KK}}$  scale, indicating that the holographic duality with QCD is mainly maintained almost below  $M_{\text{KK}}$ . This tendency of the mass spectra also denotes that such color-singlet modes beyond cutoff scale  $M_{\text{KK}}$  do not directly correspond to physical mesons in QCD. Therefore, one *cannot* manifestly conclude that the instability of the instanton only with the DBI sector really arises from the physical effect in QCD.

Furthermore, there also exists the infinite number of non-QCD modes, e.g., the Kaluza-Klein modes with large mass  $\sim O(M_{\text{KK}})$  through the Kaluza-Klein compactification of the D4 brane [3]. Therefore, if the baryon as the instanton is to be really composed by the infinite tower of the color-singlet non-QCD modes even beyond  $M_{\text{KK}}$ , there is no reason to cast away the Kaluza-Klein modes in the baryon analysis. In fact, such Kaluza-Klein modes still have the possibility to affect baryon properties, giving, e.g., the stability of the instanton even without the CS sector of the effective action of the D8 brane, though it is not to be manifestly proved yet. As a whole, there still seems to remain puzzling conflicts between the truncated-resonance model and instanton models for the baryon analyses in holographic QCD.

By looking back over the long history of hadron physics, baryons seem to have inherent difficulties being described relative to mesons. For example, the quark model succeeded in the systematic classification of the hadrons in terms of their valence quarks [65,66]. However, while the dynamics of mesons as the two-body composites can be relatively easily analyzed by solving the Bethe-Salpeter equation [67], we have to treat the complicated Faddeev equation [68] to describe the dynamics of the baryons as the three-body composites. The same difficulties are also found in the lattice QCD studies, for instance, with respect to the interquark potential of mesons [69] and baryons [70]. In fact, the quark-antiquark potential as the internal nature of the meson could be successfully measured in lattice QCD in 1980 [71], while it took almost 20 years after that to find a good measurement of the three-quark potential with the appearance of gluonic Y-type flux tube as the internal nature of the baryon [72]. The difficulty of the baryons gets more apparent in the large- $N_c$  QCD [8], which has provided a powerful perturbative treatment with the  $1/N_c$  expansion for the nonperturbative aspects of the strong interaction. In fact, large- $N_c$  QCD achieved large successes in the explanations for the hadron phenomenology, e.g., the Okubo-Zweig-Iizuka (OZI) rule [50], the  $\Delta I = 1/2$  rule [73], and the narrowness of meson resonances [8,50]. It also provided a quantitative formula for the large  $\eta'$  meson mass as the Veneziano-Witten

formula [74]. On the other hand, the baryon does not even appear as the dynamical degrees of freedom in the large- $N_c$  QCD because the baryon mass is proportional to  $O(N_c)$ . In other words,  $N_c$  quarks are needed to construct the  $SU(N_c)$  color-singlet composite as a baryon only from quarks, while a meson can still be constructed as the two-body color-singlet composite from a quark and an antiquark. In the end, the baryon appears as a “nonlocal object,” i.e., the soliton of the meson fields in the large- $N_c$  QCD. As a whole, the baryons tend to suffer from the many-body difficulties relative to the mesons by seeing the long hadron history.

Now, we suppose here that the recent baryon analyses in holographic QCD may suffer from the same kind of difficulties inherent in the baryon itself. In fact, meson properties are successfully described in the framework of holographic QCD as the Sakai-Sugimoto model [3], whereas the baryons seem to be not sufficiently described yet. One should note that the baryon mass splitting corresponds to the higher-order contributions of the large- $N_c$  expansion. In terms of the superstring theory, such baryon mass splitting corresponds to the string loop effect beyond

the classical supergravity, which is fairly intractable. These naive considerations imply that the baryon still drags the essential difficulties even by starting from the superstring theory. We have to sincerely reconsider the meaning of the difficulty existing in the baryon itself and identify an origin of the problems, which would inspire us to cure the recent conflicts of the baryon analyses in the holographic approach for the future.

## ACKNOWLEDGMENTS

Authors thank Josh Erlich and Dong-Pil Min for their communications about our truncated-resonance model as the baryon analysis in holographic QCD in comparison with the instanton models. K. N. is also indebted to Atsushi Hosaka and Hiroshi Toki for their discussions in Research Center for Nuclear Physics (RCNP). H. S. is supported by a Grant-in-Aid for Scientific Research [(C) No. 19540287] in Japan. T.K. is supported by Special Postdoctoral Research Program of RIKEN. This work is supported by the Global COE Program, “The Next Generation of Physics, Spun from Universality and Emergence.”

- 
- [1] D. Gabor, *Nature (London)* **161**, 777 (1948).
  - [2] J. M. Maldacena, *Adv. Theor. Math. Phys.* **2**, 231 (1998).
  - [3] T. Sakai and S. Sugimoto, *Prog. Theor. Phys.* **113**, 843 (2005); **114**, 1083 (2005).
  - [4] M. Bando, T. Kugo, and K. Yamawaki, *Prog. Theor. Phys.* **73**, 1541 (1985); *Phys. Rep.* **164**, 217 (1988).
  - [5] J. J. Sakurai, *Phys. Rev. Lett.* **22**, 981 (1969).
  - [6] K. Kawarabayashi and M. Suzuki, *Phys. Rev. Lett.* **16**, 255 (1966); Riazuddin and Fayyazuddin, *Phys. Rev.* **147**, 1071 (1966).
  - [7] M. Gell-Mann, D. Sharp, and W. G. Wagner, *Phys. Rev. Lett.* **8**, 261 (1962).
  - [8] G. 'tHooft, *Nucl. Phys.* **B72**, 461 (1974); **B75**, 461 (1974).
  - [9] K. Nawa, H. Suganuma, and T. Kojo, *Phys. Rev. D* **75**, 086003 (2007).
  - [10] K. Nawa, H. Suganuma, and T. Kojo, *Prog. Theor. Phys. Suppl.* **168**, 231 (2007); *Mod. Phys. Lett. A* **23**, 2364 (2008); *Prog. Theor. Phys. Suppl.* **174**, 347 (2008); H. Suganuma, K. Nawa, and T. Kojo, arXiv:0809.0805.
  - [11] H. Hata, T. Sakai, S. Sugimoto, and S. Yamato, *Prog. Theor. Phys.* **117**, 1157 (2007).
  - [12] D. K. Hong, M. Rho, H.-U. Yee, and P. Yi, *Phys. Rev. D* **76**, 061901 (2007).
  - [13] K. Hashimoto, T. Sakai, and S. Sugimoto, arXiv:0806.3122.
  - [14] H. Hata, M. Murata, and S. Yamato, *Phys. Rev. D* **78**, 086006 (2008).
  - [15] K.-Y. Kim, S.-J. Sin, and I. Zahed, *J. High Energy Phys.* **09** (2008) 001.
  - [16] T. Hatsuda and T. Kunihiro, *Phys. Rep.* **247**, 221 (1994).
  - [17] D. Bailin and A. Love, *Phys. Rep.* **107**, 325 (1984).
  - [18] K. Rajagopal and F. Wilczek, arXiv:hep-ph/0011333.
  - [19] M. Alford, K. Rajagopal, and F. Wilczek, *Phys. Lett. B* **422**, 247 (1998).
  - [20] R. Rapp, T. Schäfer, E. V. Shuryak, and M. Velkovsky, *Phys. Rev. Lett.* **81**, 53 (1998).
  - [21] K. Nawa, E. Nakano, and H. Yabu, *Phys. Rev. D* **74**, 034017 (2006).
  - [22] P. J. E. Peebles, *Principles of Physical Cosmology* (Princeton Univ. Press, Princeton, 1993).
  - [23] H. Heiselberg and M. Hjorth-Jensen, *Phys. Rep.* **328**, 237 (2000).
  - [24] M. A. Stephanov, *Proc. Sci. LAT2006* (2006) 024 [arXiv: hep-lat/0701002].
  - [25] G. S. Adkins, C. R. Nappi, and E. Witten, *Nucl. Phys.* **B228**, 552 (1983).
  - [26] I. Klebanov, *Nucl. Phys.* **B262**, 133 (1985).
  - [27] N. S. Manton and P. J. Ruback, *Phys. Lett. B* **181**, 137 (1986); N. S. Manton, *Commun. Math. Phys.* **111**, 469 (1987).
  - [28] S. Kobayashi, D. Mateos, S. Matsuura, R. C. Myers, and R. M. Thomas, *J. High Energy Phys.* **02** (2007) 016.
  - [29] C. T. Hill, *Phys. Rev. Lett.* **88**, 041601 (2002).
  - [30] H. Boschi-Filho and N. R. F. Braga, *Eur. Phys. J. C* **32**, 529 (2004); *J. High Energy Phys.* **05** (2003) 009.
  - [31] D. T. Son and M. A. Stephanov, *Phys. Rev. D* **69**, 065020 (2004).
  - [32] Y. Brihaye, C. T. Hill, and C. K. Zachos, *Phys. Rev. D* **70**, 111502 (2004).
  - [33] J. Erlich, E. Katz, D. T. Son, and M. A. Stephanov, *Phys. Rev. Lett.* **95**, 261602 (2005).
  - [34] G. F. de Teramond and S. J. Brodsky, *Phys. Rev. Lett.* **94**,

- 201601 (2005).
- [35] S. J. Brodsky and G. F. de Teramond, Phys. Rev. Lett. **96**, 201601 (2006).
- [36] A. Pomarol and A. Wulzer, J. High Energy Phys. **03** (2008) 051; Nucl. Phys. **B809**, 347 (2009).
- [37] Y. Kim, C.-H. Lee, and H.-U. Yee, Phys. Rev. D **77**, 085030 (2008).
- [38] K.-Y. Kim, S.-J. Sin, and I. Zahed, arXiv:hep-th/0608046.
- [39] N. Horigome and Y. Tanii, J. High Energy Phys. **01** (2007) 072.
- [40] D. T. Son and M. A. Stephanov, Phys. Rev. Lett. **86**, 592 (2001).
- [41] J. B. Kogut, M. A. Stephanov, and D. Toublan, Phys. Lett. B **464**, 183 (1999).
- [42] H. J. Rothe, *Lattice Gauge Theories* (World Scientific, Singapore, 1997).
- [43] K. F. Liu *et al.*, *Chiral Solitons* (World Scientific, Philadelphia, 1987).
- [44] S. Weinberg, *The Quantum Theory of Fields: Volume II: Modern Applications* (Cambridge University Press, New York, 2000), Chap. 19.
- [45] T. H. R. Skyrme, Proc. R. Soc. A **260**, 127 (1961); **262**, 237 (1961); Nucl. Phys. **31**, 556 (1962).
- [46] I. Zahed and G. E. Brown, Phys. Rep. **142**, 1 (1986).
- [47] Y. Igarashi, M. Johmura, A. Kobayashi, H. Otsu, T. Sato, and S. Sawada, Nucl. Phys. **B259**, 721 (1985); T. Fujiwara, Y. Igarashi, A. Kobayashi, H. Otsu, T. Sato, and S. Sawada, Prog. Theor. Phys. **74**, 128 (1985).
- [48] R. Rajaraman, *Solitons and Instantons* (North-Holland Publishing Company, New York, 1982).
- [49] M. Kruczenski, D. Mateos, R. C. Myers, and D. J. Winters, J. High Energy Phys. **05** (2004) 041.
- [50] E. Witten, Nucl. Phys. **B160**, 57 (1979).
- [51] T. Sakai and H. Suganuma, Phys. Lett. B **430**, 168 (1998).
- [52] W. M. Yao *et al.* (Particle Data Group), J. Phys. G **33**, 1 (2006).
- [53] C. E. DeTar and J. B. Kogut, Phys. Rev. Lett. **59**, 399 (1987).
- [54] S. Nadkarni, H. B. Nielsen, and I. Zahed, Nucl. Phys. **B253**, 308 (1985).
- [55] A. J. Niemi and G. W. Semenoff, Phys. Rep. **135**, 99 (1986).
- [56] B. L. Ioffe, Nucl. Phys. **B188**, 317 (1981); **B191**, 591(E) (1981).
- [57] B. W. Lee, *Chiral Dynamics* (Gordon and Breach, New York, 1972).
- [58] D. Jido, M. Oka, and A. Hosaka, Prog. Theor. Phys. **106**, 873 (2001).
- [59] H. Ichie, A. Hayashigaki, A. Suzuki, and M. Kimura, arXiv:nucl-th/9308017.
- [60] A. D. Jackson, A. Wirzba, and L. Castillejo, Nucl. Phys. A **486**, 634 (1988).
- [61] H. Reinhardt and B. V. Dang, Phys. Rev. D **38**, 2881 (1988).
- [62] H. Forkel, A. D. Jackson, M. Rho, C. Weiss, A. Wirzba, and H. Bang, Nucl. Phys. **A504**, 818 (1989).
- [63] N. Steenrod, *The Topology of Fibre Bundles* (Princeton University Press, Princeton, NJ, 1951).
- [64] C. Ratti, M. A. Thaler, and W. Weise, Phys. Rev. D **73**, 014019 (2006); S. Röbner, C. Ratti, and W. Weise, Phys. Rev. D **75**, 034007 (2007); C. Ratti, S. Röbner, and W. Weise, Phys. Lett. B **649**, 57 (2007); K. Fukushima, Phys. Lett. B **591**, 277 (2004).
- [65] M. Gell-Mann, Phys. Lett. **8**, 214 (1964).
- [66] G. Zweig, CERN Report No. 8182/TH 401.
- [67] H. Bethe and E. Salpeter, Phys. Rev. **82**, 60 (1951); **84**, 1232 (1951).
- [68] L. D. Faddeev, Sov. Phys. JETP **12**, 1014 (1961).
- [69] W. Lucha, F. F. Schöberl, and D. Gromes, Phys. Rep. **200**, 127 (1991).
- [70] S. Capstick and N. Isgur, Phys. Rev. D **34**, 2809 (1986).
- [71] M. Creutz, Phys. Rev. Lett. **43**, 553 (1979); **43**, 890(E) (1979); Phys. Rev. D **21**, 2308 (1980).
- [72] T. T. Takahashi *et al.*, Phys. Rev. Lett. **86**, 18 (2001); Phys. Rev. D **65**, 114509 (2002).
- [73] A. J. Buras and J. M. Gerard, Nucl. Phys. **B264**, 371 (1986); W. A. Bardeen, A. J. Buras, and J.-M. Gerard, Phys. Lett. B **180**, 133 (1986).
- [74] E. Witten, Nucl. Phys. **B149**, 285 (1979); **B156**, 269 (1979); G. Veneziano, Nucl. Phys. **B159**, 213 (1979).